

# Non-autonomous bright-dark solitons and Rabi oscillations in multi-component Bose-Einstein condensates

T Kanna<sup>1</sup>, R Babu Mareeswaran<sup>1</sup>, F Tzitoura<sup>2</sup>, H E Nistazakis<sup>2</sup>  
and D J Frantzeskakis<sup>2</sup>

<sup>1</sup>Post Graduate and Research Department of Physics, Bishop Heber College,  
Tiruchirapalli-620 017, Tamil Nadu, India

<sup>2</sup>Department of Physics, University of Athens, Panepistimiopolis, Zografos, Athens  
15784, Greece

E-mail: kanna\_phy@bhc.edu.in (corresponding author), dfrantz@phys.uoa.gr

**Abstract.** We study the dynamics of non-autonomous bright-dark matter-wave solitons in two- and three- component Bose-Einstein condensates. Our setting includes a time-dependent parabolic potential and scattering length, as well as Rabi coupling of the separate hyperfine states. By means of a similarity transformation, we transform the non-autonomous coupled Gross-Pitaevskii equations into the completely integrable Manakov model with defocusing nonlinearity, and construct the explicit form of the non-autonomous soliton solutions. The propagation characteristics for the one-soliton state, and collision scenarios for multiple soliton states are discussed in detail for two types of time-dependent nonlinearities: a kink-like one and a periodically modulated one, with appropriate time-dependence of the trapping potential. We find that in the two-component condensates the nature of soliton propagation is determined predominantly by the nature of the nonlinearity, as well as the temporal modulation of the harmonic potential; switching in this setting is essentially due to Rabi coupling. We also perform direct numerical simulation of the non-autonomous two-component coupled Gross-Pitaevskii equations to corroborate our analytical predictions. More interestingly, in the case of the three-component condensates, we find that the solitons can lead to collision-induced energy switching (energy-sharing collision), that can be profitably used to control Rabi switching or vice-versa. An interesting possibility of reversal of the nature of the constituent soliton, i.e., bright (dark) into dark (bright) due to Rabi coupling is demonstrated in the three-component setting.

PACS numbers: 03.75.Mn, 03.75.Lm, 02.30.Ik

Journal Reference: *J. Phys. A: Math. Theor.* **46** (2013) 475201

## 1. Introduction

Studies on atomic Bose-Einstein condensates (BECs) have received considerable attention in recent years [1]. In this context, it has been shown that nonlinear effects in matter waves can emerge, with this particular direction having attracted much interest both in theory and in experiments [2,3]. From a theoretical viewpoint, this interest arises from the fact that many of such nonlinear effects can be understood in the framework of lowest-order mean-field theory, namely by means of the so-called Gross-Pitaevskii equation (GPE), which is nothing but the ubiquitous nonlinear Schrödinger (NLS) equation with external potential [1–3]. The GPE is a nonlinear evolution equation (with the nonlinearity originating from the interatomic interactions) and, as such, it permits the study of a variety of interesting purely nonlinear phenomena. The latter, have primarily been studied by treating the condensate as a purely nonlinear coherent matter-wave, i.e., from the viewpoint of the dynamics of nonlinear waves. Relevant studies have already been summarized in various books [2] and reviews; see, e.g., [4] for bright solitons, [5] for dark solitons, [6] for vortices, [7] for dynamical instabilities in BECs, and so on.

The formation and dynamical properties of solitons in BECs are determined by the nature of their two-body atomic interactions, i.e., the sign of the *s*-wave scattering length which may be positive (negative) for repulsive (attractive) inter-atomic interactions. For instance, atomic dark (bright) solitons are formed in condensates with repulsive (attractive) interactions [2–5] (note that bright gap solitons are also possible in repulsive BECs, but those are critically formed due to the presence of a periodic—optical lattice—potential [8]). On the other hand, it should be stressed that the above conditions can dramatically change in the case of *multi-component* BECs, composed by two or more different hyperfine states of the same atom species (e.g.,  $^{87}\text{Rb}$ ) [9, 10]: in such a case, e.g., binary condensates with repulsive inter- and intra-species interactions can support mixed bright-dark (BD) solitons. This type of vector soliton consists of a dark soliton in one component coupled to a bright soliton in the second component. These solitons are usually referred to as “symbiotic” solitons, because the bright component cannot be supported in a stand-alone fashion (it is only supported as such in attractive BECs [4]; see also [5]), and is only sustained because of the presence of its dark counterpart, which acts as an effective external trapping potential. Such atomic BD solitons were predicted in theory [11] and observed in experiments from different experimental groups [12–14]. Notice that solitons in three-component condensates (e.g., spinor  $F = 1$  BECs) have been studied too [15–17] and mixed, BD solitons were predicted to occur as well [18].

On the other hand, coming back to the role of the sign and magnitude of the scattering length, it is important to note that they can be adjusted over a relatively large range by employing external magnetic, electric or optical fields near Feshbach resonances [19]. This possibility has given rise to many theoretical and experimental studies, with a prominent example being the formation of bright matter-wave solitons and soliton trains in attractive condensates [20], by switching the interatomic interactions from repulsive

to attractive. Many theoretical works studied the BEC dynamics under temporal modulation of the nonlinearity. In particular, the application of such a “Feshbach resonance management” (FRM) technique [21] can be used to stabilize attractive higher-dimensional BEC against collapse [22], to create robust matter-wave breathers in the effectively one-dimensional (1D) condensate [21, 23], or compress bright solitons in the presence of expulsive potentials [24]. Mathematically speaking, if the scattering length is time dependent then so does the nonlinearity coefficient in the GPE, and the latter becomes *non-autonomous*. In the pioneering works [25], it has been shown that the single-component non-autonomous GPE can be transformed into the standard integrable NLS equation. The procedure developed in Ref. [25] can be generalized to two-component condensates [26] and the corresponding non-autonomous matter-wave solitons were studied extensively with aid of the explicit soliton solutions reported in Refs. [27–29].

This work deals with the dynamics of multi-component BECs, particularly two- and three-component BECs, with temporally modulated scattering length and trapping potential, and in the presence of Rabi coupling; the latter is accounted for by a linear coupling between separate wave functions induced by a radio frequency [9] (see also Refs. [30–32] for a theoretical analysis and applications). Recently, coherent many body Rabi oscillations have been observed experimentally and theoretically discussed in Ref. [33]. Using two successive transformations, with one constraint equation being in the form of a Ricatti equation, we reduce the original multicomponent non-autonomous GPEs to the integrable defocusing vector NLS equation, known as the Manakov model [34]. These transformations can be viewed as a rotation followed by a similarity transformation. This way, we find non-autonomous mixed (BD) solitons and analyze their dynamics and interactions in detail, in both two- and three-component settings. We find that in the two-component system, soliton propagation is determined predominantly by the nature of the nonlinearity, as well as the temporal modulation of the harmonic potential; switching in this setting is essentially due to Rabi coupling. Our analytical predictions are corroborated with results from direct simulations; very good agreement between the two is found. Then by going one step further in the case of the three-component system, we find that the solitons can lead to collision-induced energy switching (energy-sharing collision) that can be profitably used to control Rabi switching or vice-versa. An interesting possibility of reversal of the nature of the constituent soliton, i.e., bright (dark) into dark (bright) induced by the Rabi coupling is demonstrated in the three-component setting.

The remaining part of this paper is arranged as follows. In Sec. II, we introduce the generalized non-autonomous coupled GPEs, for two-component condensates, with time-varying interaction strength and Rabi coupling. Also, we construct the one- and two-soliton solutions to the 1D coupled non-autonomous GPEs and analyze their propagation characteristics. In Sec. III, we consider the three-component non-autonomous GPEs with Rabi coupling, and explore the interesting energy exchange collisional features of non-autonomous matter-wave solitons. Finally, in Sec. IV, we present our conclusions.

## 2. Non-autonomous BD solitons in two-component BECs and Rabi oscillations

In the mean field approximation, the dynamics of two-component condensates can be well described by a pair of two coupled three-dimensional (3D) GPEs (see, e.g., Ref. [35]). In the physically relevant case of highly anisotropic (cigar-shaped) traps, these GPEs can be reduced to an effectively 1D system (see, e.g., Ref. [3]), which is of the following dimensionless form:

$$i\psi_{j,t} = -\frac{1}{2}\psi_{j,xx} + \sum_{l=1}^2 g_{jl}(t)|\psi_l|^2\psi_j + \sum_{l=1, (l \neq j)}^2 \sigma_l \psi_l + V_j(x, t)\psi_j, \quad j = 1, 2. \quad (1)$$

Here,  $\psi_j$  is the macroscopic wave function of the  $j^{\text{th}}$  component, time  $t$  and spatial coordinate  $x$  are respectively measured in units of the inverse transversal frequency  $\omega_{\perp}^{-1}$  and the transverse harmonic oscillator length  $a_0 = \sqrt{\hbar/m\omega_{\perp}}$  ( $m$  denotes atomic mass). In Eq. (1) the nonlinearity coefficients  $g_{jl}$  are proportional to the  $s$ -wave scattering lengths  $a_{jl}$ , namely  $g_{jl}(t) = 2a_{jl}(t)/a_B$  (where  $a_B$  is the Bohr radius), and are assumed to be subject to the FRM technique (see below); furthermore  $V_j(x, t)$  are the external potentials [for  $V(x, t) < 0$  ( $V(x, t) > 0$ ) the potential is expulsive (confining)], and the linear cross coupling parameters  $\sigma_l$  represent the Rabi coupling: in fact these coefficients are proportional to the Rabi frequency, and are responsible for the transfer of atoms of component  $\psi_1$  to component  $\psi_2$  and vice-versa. In our case, considering two different hyperfine states of the same atom, the external time-varying potentials  $V_j$  are equal, i.e.,  $V_1 = V_2 = V = (1/2)\Omega^2(t)x^2$ . Here, the strength of the parabolic trap is given by  $\Omega^2(t) = \omega_x^2(t)/\omega_{\perp}^2$ , where  $\omega_x(t)$  is the temporally modulated axial trap frequency. Finally, the macroscopic wave functions  $\psi_j$  are normalized such that  $\int_{-\infty}^{\infty} |\psi_j|^2 dx = N_j$  ( $j = 1, 2$ ), where  $N_j$  is the number of atoms in the  $j^{\text{th}}$  component.

### 2.1. Non-autonomous BD one-soliton solution

Based on experimental results pertaining to two-component  $^{87}\text{Rb}$  BECs (see, e.g., [13]), we can assume that the scattering length ratios are almost equal to one, and also they can be tuned through Feshbach resonance (as it was demonstrated in the experimental works [36,37]). Hence, we consider the case of equal interaction strengths, i.e.,  $g_{jl} = \rho(t)$  in Eq. (1), and choose the linear coupling coefficients  $\sigma_l$  as  $\sigma_1 = \sigma_2 = \sigma$ , with  $\sigma > 0$ .

In such a case, as shown in Appendix A, we can use two successive transformations to map the non-autonomous system (1) into an integrable autonomous nonlinear system. This is possible mainly due to the temporal dependence of the nonlinearity and external harmonic potential; in the absence of such dependence these transformations are not possible, in general. Notice, however, that in the absence of potential (homogeneous system), one can transform Eq. (1) into an integrable coupled nonlinear Schrödinger (CNLS) system even in the absence of inhomogeneities. The above mentioned transformations are: (i) a unitary transformation (see, e.g., Refs. [30, 32]) to reduce Eq. (1) to a non-autonomous system of equations without the Rabi coupling term; (ii)

a similarity transformation, which reduces the aforementioned system to the following integrable defocusing CNLS equations [38, 39]:

$$iq_{j,T} + q_{j,XX} - 2 \sum_{l=1}^2 |q_l|^2 q_j = 0, \quad j = 1, 2. \quad (2)$$

Equation (2) is the completely integrable Manakov system and admits  $N$ -soliton solutions of dark-dark and mixed (BD) types. Here, we focus only on mixed type soliton solutions due to their recent experimental observations and for their special dynamical features [12, 13].

The mixed one-soliton solution of Eq. (2) can be obtained by Hirota's direct method [41]. In standard form, the mixed one-soliton solution of the two-component defocusing CNLS equations with the bright (dark) part appearing in the  $q_1$  ( $q_2$ ) component (see Refs. [27, 39]) is given in Appendix B.1. Using the analytical form of this type of soliton, as well as the transformations of Appendix A, we find an exact analytical non-autonomous soliton solution of Eq. (1) in the form:

$$\psi_1 = \cos(\sigma t)\phi_1 - i \sin(\sigma t)\phi_2, \quad \psi_2 = \cos(\sigma t)\phi_2 - i \sin(\sigma t)\phi_1, \quad (3)$$

where  $\phi_1$  and  $\phi_2$  are given by:

$$\begin{aligned} \phi_1(x, t) &= \xi_1 \sqrt{2\rho(|c_1|^2 \cos^2 \varphi_1 - k_{1R}^2)} e^{i(\bar{\eta}_{1I} + \theta + \bar{\theta})} \\ &\times \operatorname{sech} \left( k_{1R}(\sqrt{2} \xi_1(\rho x - 2\xi_2 \xi_1^2 \int_0^t \rho^2 dt) - 2k_{1I} \xi_1^2 \int_0^t \rho^2 dt) + R/2 \right), \end{aligned} \quad (4)$$

$$\begin{aligned} \phi_2(x, t) &= -c_1 \xi_1 \sqrt{2\rho} e^{i(\bar{\zeta}_1 + \varphi_1 + \bar{\theta})} \\ &\times \left( \cos \varphi_1 \tanh[k_{1R}(\sqrt{2} \xi_1(\rho x - 2\xi_2 \xi_1^2 \int_0^t \rho^2 dt) - 2k_{1I} \xi_1^2 \int_0^t \rho^2 dt) + R/2] + i \sin \varphi_1 \right), \end{aligned} \quad (5)$$

where  $\bar{\eta}_{1I} = k_{1I} \sqrt{2} \xi_1(\rho x - 2\xi_2 \xi_1^2 \int_0^t \rho^2 dt) - (k_{1R}^2 - k_{1I}^2 - 2|c_1|^2) \xi_1^2 \int_0^t \rho^2 dt$ ,  $\bar{\zeta}_1 = -(b_1^2 + 2|c_1|^2) \xi_1^2 \int_0^t \rho^2 dt + b_1 \sqrt{2} \xi_1(\rho x - 2\xi_2 \xi_1^2 \int_0^t \rho^2 dt)$  and the other parameters and functions involved in the above equations are defined in Appendices A and B.

The above mixed soliton bears resemblance to the recently observed, so-called ‘‘beating’’ dark-dark soliton [14, 42], where the bright and dark parts coexist in the same component with a constant asymptotic value as  $|x| \rightarrow \infty$ ; however, the form of this BD soliton still depends on the Rabi coupling and the time-dependent nonlinearity and parabolic potential. Notice that due to the presence of Rabi coupling, there will be a periodic switching between the two components along with oscillating background. Another important observation for the integrable two-component case is the dependence of the existence of e.g., the bright part of the mixed soliton on its dark counterpart (see Eqs. (B.1)-(B.2) and relevant discussion in Appendix B.1). Thus, it is impossible to make any one of the constituents (bright/dark) of the mixed soliton to vanish completely. In fact, this will result in singularities in the other soliton part. This holds even in the presence of the Rabi coupling for the two-component system.

To elucidate the dynamics of such special type of mixed soliton we consider the following two examples.

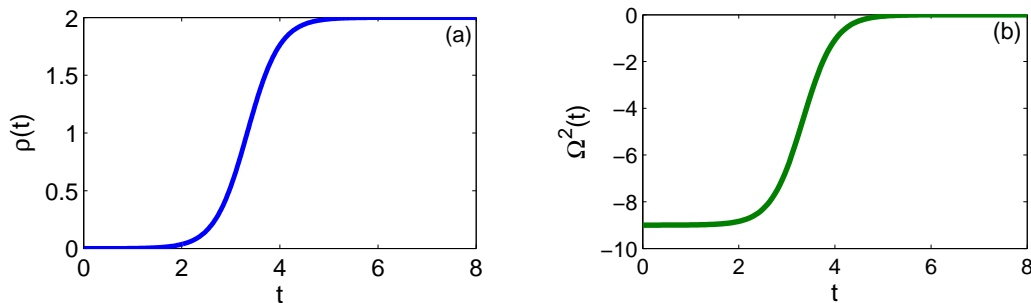


**Figure 1.** Typical form of the kink-like nonlinearity  $\rho(t)$  (a) and corresponding strength of external harmonic potential (b).

### Example 1: Kink-like nonlinearity

First we note that a fast time modulated nonlinearity displays interesting dynamics in BECs [43]. A relatively sudden jump in the nonlinearity coefficient can be well represented by a kink-like nonlinearity of the form:

$$\rho(t) = 1 + \tanh(\omega t + \delta), \quad (6a)$$

with the associated atomic scattering length being  $a_s(t) = \frac{1}{2}a_B[1 + \tanh(\omega t + \delta)]$ ; here,  $\omega$  denotes the time scale characterizing the jump, and  $\delta$  is an arbitrary constant.

This is shown in Fig. 1(a) and the corresponding external harmonic potential is displayed in Fig. 1(b). The time-dependent nonlinearity  $\rho(t)$  admitting the above form can be realized for the following scattering length [25],

$$\frac{a_s(t)}{a_{bg}} = \left( 1 + \frac{\Delta}{B_0 - B(t)} \right), \quad (6b)$$

where  $a_{bg}$  is the value of scattering length far from the Feshbach resonance,  $B(t)$  is the applied time-varying magnetic field,  $B_0$  is the resonant value of the magnetic field, and  $\Delta$  is the resonance width in the presence of the magnetic field. The corresponding strength of the time-dependent magnetic trap is determined by a Riccati equation [see Eq. (A.8) in Appendix A] as follows:

$$\Omega^2(t) = - \left( \frac{4\omega^2}{1 + e^{2(\omega t + \delta)}} \right). \quad (6c)$$

The propagation of the non-autonomous mixed soliton in the absence and presence of Rabi coupling are depicted in the top panels of Figs. 2 and 3, respectively. We have also solved the system (1) numerically by means of the split-step Fourier method, and the resulting numerical plots for the above choice of the time-dependent nonlinearity and potential strength (6c) are given in the bottom panel.

Comparing the top and bottom panels, one can see that there is a very good agreement between numerical and analytical results. We find that, in the absence of the Rabi coupling, there are no oscillations for the solitons and the background. However, the shape, width and velocity of solitons are modulated. Then, the introduction of Rabi term leads to an exchange of number of atoms between the components, which

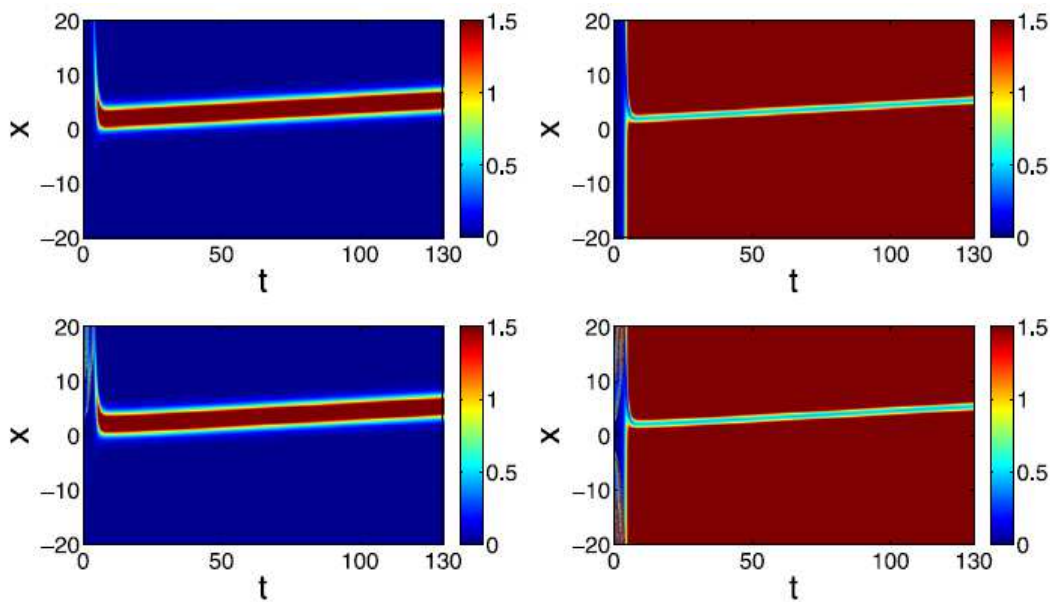


**Figure 2.** Two-component one-soliton solution of GPEs. (1) with kink-like nonlinearity in the absence of Rabi coupling. Top panels show the intensity plots of exact analytical results (upper left panel: bright component, and right upper panel: dark component of the mixed soliton), while bottom panels show numerical results (left bottom panel: bright component, and right bottom panel: dark component of the mixed soliton). The parameter values are  $k_1 = 0.5 + 0.02i$ ,  $b_1 = 0.2$ ,  $c_1 = 2$ ,  $\xi_1 = 0.5$ ,  $\xi_2 = 0$ ,  $\alpha_1^{(1)} = 0.5$ ,  $\delta = -4$  and  $\omega = 0.7$ .

ultimately results in beating oscillations, as shown in Fig. 3. For small values of  $\sigma$ , the background just starts to oscillate (see Fig. 3). However, by increasing the parameter  $\sigma$ , one can observe rapid oscillations of the background also. To illustrate this, the contour plots of  $|\psi_1|^2$  for  $\sigma = 0.1$  and  $\sigma = 0.2$  are shown in Fig. 4. Similar observations can be made for the second component, ( $\psi_2$ ), as well. These oscillations of the background are due to the exchange of condensates between the soliton and the background.

Another important observation following from Figs. 3 and 4, as well as from expressions (3)-(5) is that the increase of the value of Rabi coupling leads a significant portion of the dark part of mixed soliton to appear in the first component ( $\psi_1$ ), along with the bright part accompanied by beating effects. Similar effects take place in component  $\psi_2$  too. Thus, in a given component one can have co-existing oscillating BD soliton.

Enlarging Fig. 3 in the region  $t = 0$  to 5, we observe that the non-autonomous mixed soliton is absent in this region. This is due to the form of the nonlinearity  $\rho(t)$ , which becomes zero in the range  $t = 0$  to 5 and reaches a saturation for large positive  $t$  values. Thus, even though the Rabi coupling leads to an exchange of atoms among the two components leading to oscillations, the nature of soliton propagation is predominantly determined by the nature of time-dependent nonlinearity.

### Example 2: Periodically modulated nonlinearity

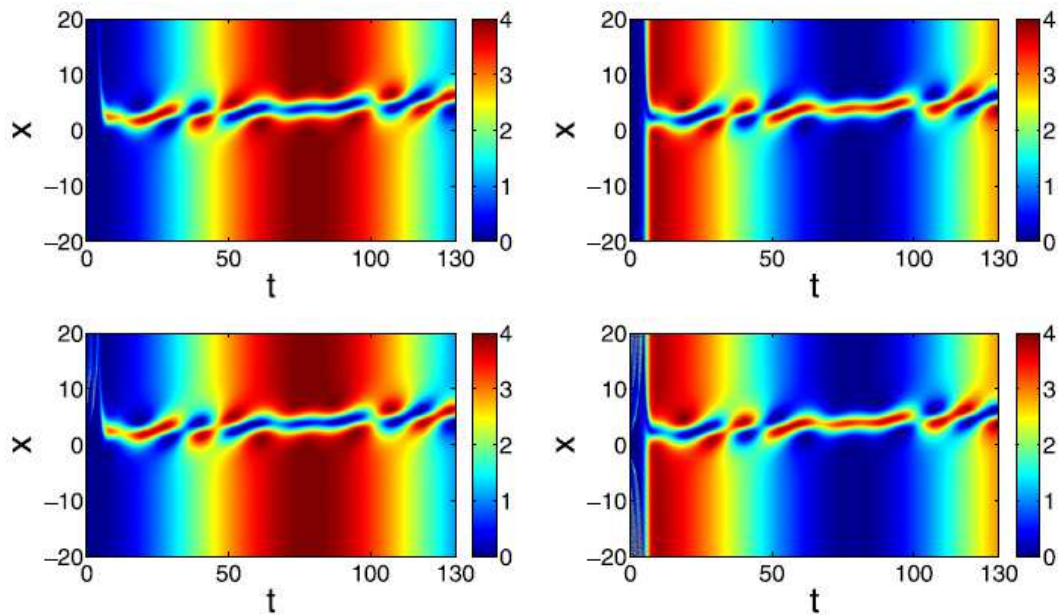


**Figure 3.** Two-component mixed one-soliton solution with co-existing bright-dark parts for the kink-like nonlinearity in the presence of Rabi coupling: Analytical results (upper left panel:  $\psi_1$  component, and right upper panel:  $\psi_2$  component of the mixed soliton). Numerical results (left bottom panel:  $\psi_1$  component, and right bottom panel:  $\psi_2$  component of the mixed soliton). The parameter values are  $k_1 = 0.5 + 0.02i$ ,  $b_1 = 0.2$ ,  $c_1=2$ ,  $\xi_1 = 0.5$ ,  $\xi_2 = 0$ ,  $\alpha_1^{(1)} = 0.5$ ,  $\delta = -4$ ,  $\omega = 0.7$  and  $\sigma = 0.02$ .

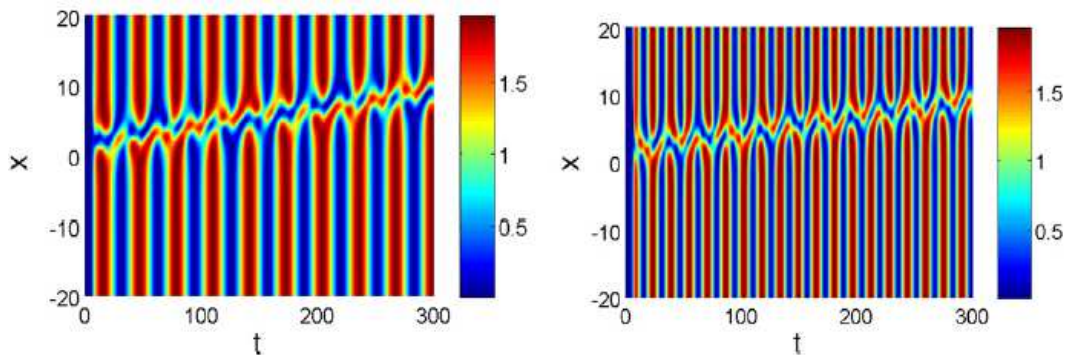


**Figure 4.** Mixed one-soliton solution for the kink-like nonlinearity in left panel for  $\sigma = 0.1$  and right panel for  $\sigma = 0.2$ . The other parameters are fixed as  $k_1 = 0.5 + 0.02i$ ,  $b_1 = 0.2$ ,  $\xi_1 = 0.5$ ,  $\xi_2 = 0$ ,  $\alpha_1^{(1)} = 0.5$ ,  $\delta = -4$  and  $\omega = 0.7$ .

Next, we consider another physically interesting example, namely the case of a periodic time-varying nonlinearity of the form:

$$\rho(t) = 1 + \varepsilon \cos(\omega t + \delta), \quad (7a)$$

where  $\varepsilon$  is an arbitrary real constant,  $\omega$  is the characteristic frequency, and  $\delta$  is a real constant parameter. In this case, the form of atomic scattering length is  $a_s(t) = \frac{1}{2}a_B[1 + \varepsilon \cos(\omega t + \delta)]$ . Figure 5(a) represents the form of such a time-varying nonlinearity. The expression for the pertinent time-dependent external magnetic field



$B(t)$  required to achieve the above form of the nonlinearity can be determined from the formula (6b). The corresponding strength of the magnetic trap admits the form

$$\Omega^2(t) = \omega^2 \varepsilon \left( \frac{-3\varepsilon - 2\cos(\omega t + \delta) + \varepsilon \cos[2(\omega t + \delta)]}{2[1 + \varepsilon \cos(\omega t + \delta)]^2} \right), \quad (7b)$$

in order to satisfy Eq. (A.8). Note that the potential is sign reversible and can support the same type of soliton for both positive and negative signs; see Fig. 5(b).

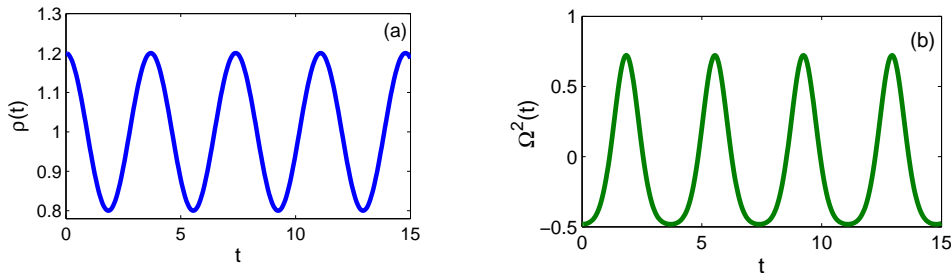


**Figure 5.** Periodically modulated nonlinearity  $\rho(t)$  (a) and corresponding strength of the external harmonic potential (b).

It is apparent from the periodic nature of the nonlinearity, and the time modulation of the strength of the external potential, that the condensates also execute periodic oscillations in both the components even in the absence of linear coupling as shown in Fig. 6. The numerical results, obtained by a direct integration of Eq. (1) are shown in the bottom panel of Fig. 6 in the absence of Rabi coupling. Next, we introduce the Rabi coupling between the two components; then, as expected, there will be an exchange of atoms between the components, as well as between the soliton and the background. This exchange induces oscillations in the density of condensates which, in turn, modulate the oscillations due to the periodic nature of  $\rho(t)$  and  $\Omega^2(t)$  and result in soliton beating in both components. This becomes clear in Fig. 7, from the plots showing the non-autonomous soliton (3) for the choice (7a) (upper panel) and the corresponding numerical results (bottom panel).

As in the previous example, here also both parts of the mixed soliton co-exist in a given component due to Rabi switching. The left panel of Fig. 8 displays the propagation of mixed soliton for a small value of  $\sigma$  ( $=0.1$ ). It is observed that the soliton only oscillates periodically, but the background is not oscillating. The right panel of Fig. 8 displays that for larger value of  $\sigma$  (say  $\sigma = 0.2$ ), the background oscillates rapidly and significant switching of dark and bright parts among the components occurs, thereby resulting in the co-existence of both dark and bright parts in the same component. By increasing the values of  $\omega$ , we also observe “creeping” soliton propagation with beating effects, which are not presented here. Similar type of creeping soliton appears in the presence of inhomogeneities too.

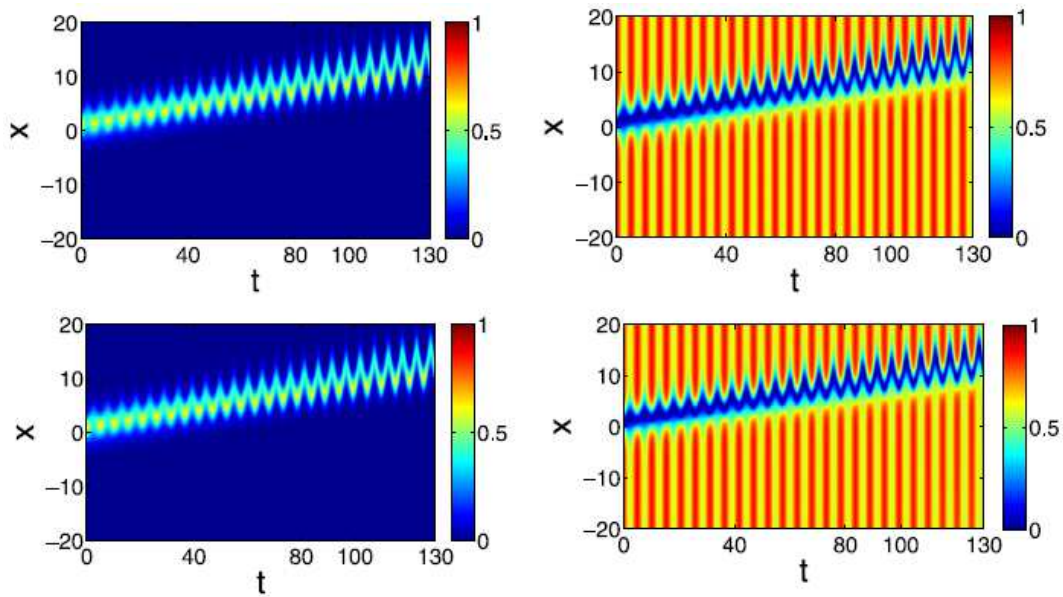


**Figure 6.** Two component mixed one-soliton solution of Eq. (1) for the periodically modulated nonlinearity in the absence of Rabi coupling. Top panels show the exact analytical results (upper left panel: bright component, and right upper panel: dark component) and bottom panels show numerical results (left bottom panel: bright component, and right bottom panel: dark component). The parameter values are  $k_1 = 0.5 + 0.1i$ ,  $b_1 = 0.2$ ,  $\alpha_1^{(1)} = 1.5$ ,  $c_1 = 1$ ,  $\xi_1 = 0.6$ ,  $\xi_2 = 0$ ,  $\varepsilon = 0.2$ ,  $\omega = 1.2$  and  $\delta = 0$ .

From the above two examples, we can conclude that in the non-autonomous two-component GPEs, (1) the nature of soliton propagation is determined predominantly by the temporal dependence of  $\rho(t)$  and  $\Omega^2(t)$  while the switching of condensates is completely dependent on the Rabi coupling.

## 2.2. Two soliton solution of non-autonomous two-component GPEs

We now turn our attention to the case of mixed two-soliton solution of the integrable 2-CNLS system (2). The explicit form of this solution, given in Appendix B.1, contains all the information regarding the collision of two solitons. We will employ this autonomous soliton solution to construct the exact two soliton solution of the corresponding non-autonomous system (1) in detail.

The asymptotic analysis of the two-soliton solution of the two component GPEs system (2) given in Appendix C.1, shows that the two solitons undergo standard elastic collision as  $|A_i^{l+}| = |A_i^{l-}|$ ,  $i, l = 1, 2$ , where  $A_i^l$  represents the amplitude of  $l^{\text{th}}$  soliton in  $i^{\text{th}}$  component. Here and in the following, the superscript (subscript) of A (or  $\psi$ ) represents the number of soliton (component) while  $-(+)$  appearing in the corresponding quantities indicates their form before (after) collision. Thus the amplitude and speed of the bright and dark components are preserved after the collision, except for a phase-shift ( $\Phi = \frac{R_3 - R_2 - R_1}{2}$ ), where  $R_1, R_2$  and  $R_3$  are defined in Appendix B.1. This elastic

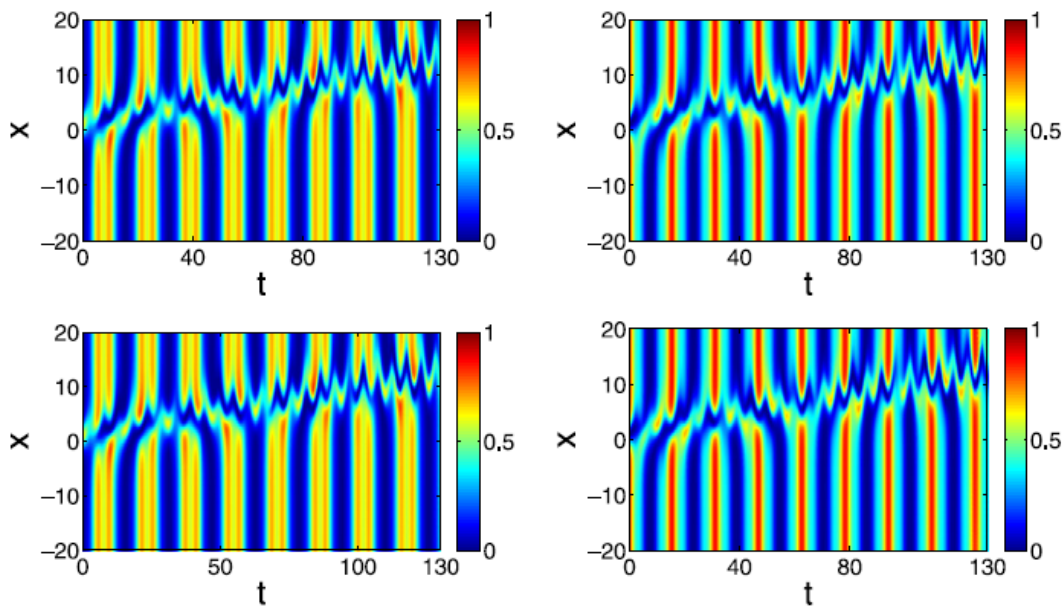


**Figure 7.** Two component one-soliton solution of Eq. (1) for the periodically modulated nonlinearity in the presence of Rabi switch. Top panels show the exact analytical results (upper left panel:  $\psi_1$  component, and right upper panel:  $\psi_2$  component) and bottom panels the numerical results (left bottom panel:  $\psi_1$  component, and right bottom panel:  $\psi_2$  component). The parameter values are  $k_1 = 0.5 + 0.1i$ ,  $b_1 = 0.2$ ,  $\alpha_1^{(1)} = 1.5$ ,  $c_1 = 1$ ,  $\xi_1 = 0.6$ ,  $\xi_2 = 0$ ,  $\varepsilon = 0.2$ ,  $\omega = 1.2$ ,  $\delta = 0$  and  $\sigma = 0.2$ .

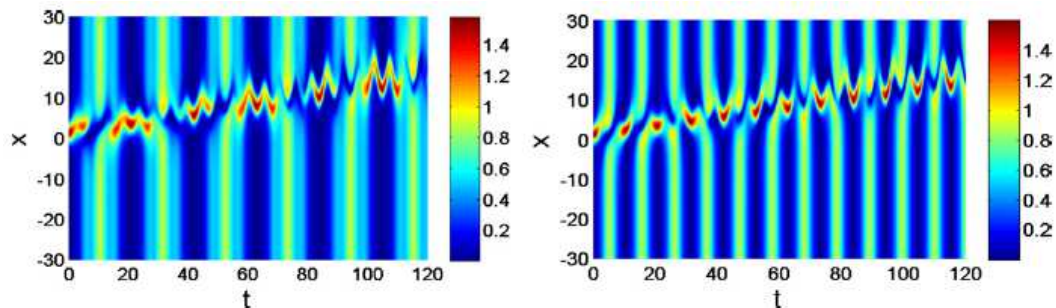


**Figure 8.** Intensity plots of non-autonomous one-soliton solution in the  $\psi_1$ -component [see Eq. 7(a)] for the periodically modulated nonlinearity for  $\sigma = 0.1$  (left panel) and  $\sigma = 0.2$  (right panel). The other parameters are fixed as  $k_1 = 0.5 + 0.1i$ ,  $b_1 = 0.2$ ,  $\alpha_1^{(1)} = 1.5$ ,  $c_1 = 1.5$ ,  $\xi_1 = 0.6$ ,  $\xi_2 = 0$ ,  $\varepsilon = 0.2$ ,  $\omega = 1.2$  and  $\delta = 0$ .

collision of solitons is shown in Fig. 9.

The exact dynamics of the non-autonomous two mixed solitons can be understood after transforming the two-soliton solution [see Eqs. (B.3)-(B.13)] by using the transformations given in Appendix A [see Eqs. (A.4) and (A.1)]. In the following analysis, the collision dynamics for two interesting forms of the nonlinearity coefficient  $\rho(t)$ , namely kink-like and the periodically modulated nonlinearity are considered in detail.

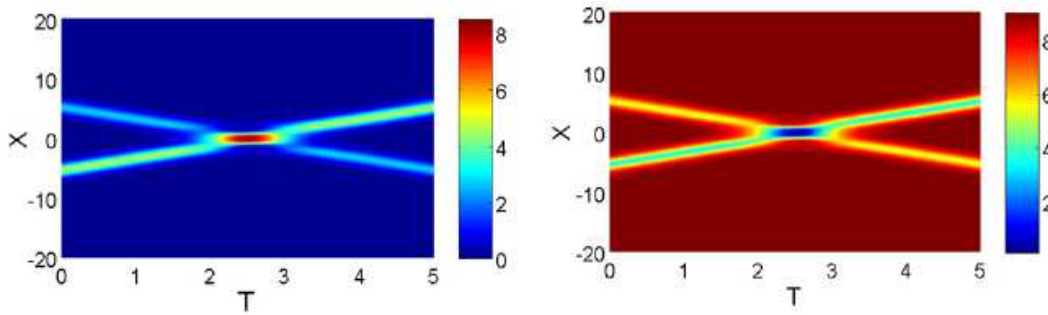


**Figure 9.** Two soliton collision of system (2) [see Eq. (B.4)]. The soliton parameters are fixed as  $k_1 = -1 + i$ ,  $k_2 = 1 - i$ ,  $c_1 = 3$ ,  $b_1 = 0.2$  and  $\alpha_1^{(1)} = \alpha_2^{(1)} = 0.02$ .

(i) *Collision dynamics in the presence of kink-like modulated nonlinearity*

Figure 10 shows the two-soliton collision in the non-autonomous two-component GPEs (1) with kink-like nonlinearity, whose form is given by Eq. (6a) in the absence of Rabi terms, and the corresponding strength of the magnetic trap is given by Eq. (6c). The figure shows that the two solitons undergo a collision around  $t = 80$  and get well separated for larger values of  $t$ . Next, we include the Rabi coupling and plot the non-

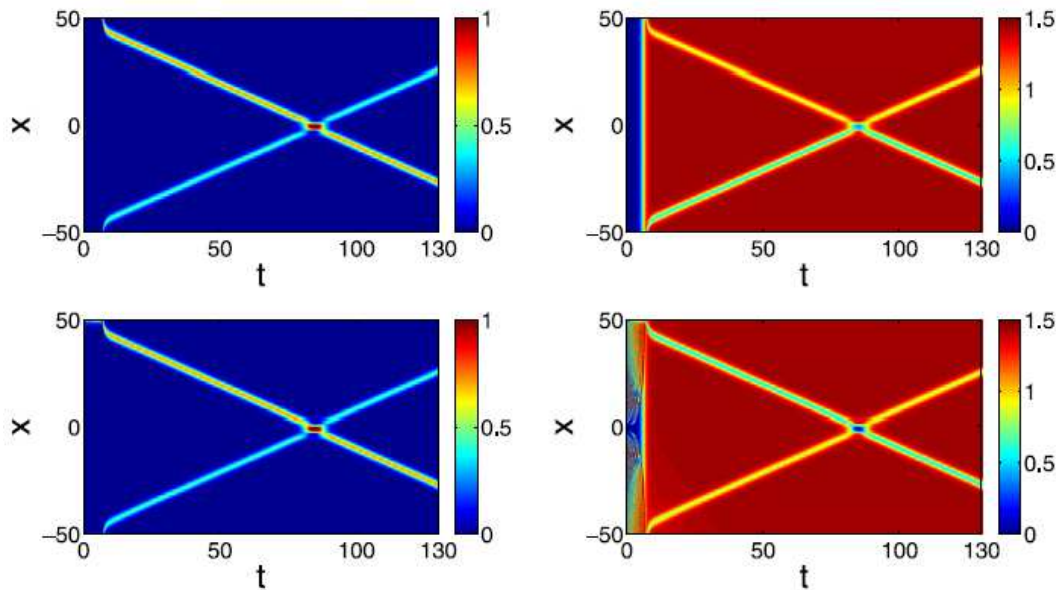


**Figure 10.** Interaction of non-autonomous solitons in two-component GPEs for the kink-like nonlinearity in the absence of Rabi coupling. Top panels show the analytical results (upper left panel: bright component, and right upper panel: dark component) and bottom panels show the numerical results (left bottom panel: bright component, and right bottom panel: dark component). The soliton parameters are  $k_1 = -1 + i$ ,  $k_2 = 1 - i$ ,  $c_1 = 3$ ,  $b_1 = 0.2$ ,  $\alpha_1^{(1)} = \alpha_2^{(1)} = 0.03$ ,  $\delta = -4.5$ ,  $\xi_1 = 0.2$ ,  $\xi_2 = 0$  and  $\omega = 0.75$ .

autonomous two soliton collision in Fig. 11. We notice from Figs. 10 and 11 that the nature of soliton collision in the presence of Rabi term looks alike the soliton collision

in the absence of Rabi term. Additionally, in the present case, there is an oscillating exchange of atoms between the two components. The background oscillates in a periodic manner, in which the oscillations in a given component is maximum while it is minimum in the other.

Here we present the asymptotic analysis of the non-autonomous two-soliton solution of two-component GPEs with kink-like nonlinearity, obtained by making use of (B.3)-(B.13) and the transformations (A.1) and (A.4). For the choice  $k_{1R} < k_{2R}$ ,  $k_{1I} > k_{2I}$ , the asymptotic forms of the non-autonomous solitons ( $S_l$ ,  $l = 1, 2$ ) well before and after collision can be expressed as below:

#### Before collision

$$\begin{aligned} \psi_1^{l-} &= \xi_1 \sqrt{2\rho} [A_1^{l-} \cos(\sigma t) \operatorname{sech}(\eta_{lR} + R_l/2) e^{i(\eta_{lI} + \tilde{\theta})} \\ &\quad - i A_2^{l-} \sin(\sigma t) (\cos\varphi_l \tanh(\eta_{lR} + R_l/2) + i \sin\varphi_l)], \end{aligned} \quad (8)$$

$$\begin{aligned} \psi_2^{l-} &= \xi_1 \sqrt{2\rho} [A_2^{l-} \cos(\sigma t) (\cos\varphi_l \tanh(\eta_{lR} + R_l/2) + i \sin\varphi_l), \\ &\quad - i A_1^{l-} \sin(\sigma t) \operatorname{sech}(\eta_{lR} + R_l/2) e^{i(\eta_{lI} + \tilde{\theta})}], \quad l = 1, 2, \end{aligned} \quad (9)$$

#### After collision

$$\begin{aligned} \psi_1^{l+} &= \xi_1 \sqrt{2\rho} [A_1^{l+} \cos(\sigma t) \operatorname{sech}(\eta_{lR} + (R_3 - R_{3-l})/2) e^{i(\eta_{lI} + \tilde{\theta})} \\ &\quad - i A_2^{l+} \sin(\sigma t) (\cos\varphi_l \tanh(\eta_{lR} + (R_3 - R_{3-l})/2) + i \sin\varphi_l)], \end{aligned} \quad (10)$$

$$\begin{aligned} \psi_2^{l+} &= \xi_1 \sqrt{2\rho} [A_2^{l+} \cos(\sigma t) (\cos\varphi_l \tanh(\eta_{lR} + (R_3 - R_{3-l})/2) + i \sin\varphi_l)] \\ &\quad - i A_1^{l+} \sin(\sigma t) \operatorname{sech}(\eta_{lR} + (R_3 - R_{3-l})/2) e^{i(\eta_{lI} + \tilde{\theta})}], \quad l = 1, 2, \end{aligned} \quad (11)$$

where  $A_1^{l-} = \alpha_l^{(1)} e^{-\frac{R_l}{2}}$ ,  $A_2^{l-} = -c_1 e^{i(\zeta_1 + \varphi_l + \tilde{\theta})}$ ,  $A_1^{l+} = \frac{1}{2} e^{(2\delta_{l1} - R_3 - R_{3-l})/2}$ ,  $A_2^{l+} = c_1 e^{i(\zeta_1 + 2\varphi_{3-l} + \varphi_l + \tilde{\theta})}$ ,  $\rho = 1 + \tanh(\omega t + \delta)$ ,  $\eta_{lR} = k_{lR} (\sqrt{2} \xi_1 (\rho x - 2\xi_2 \xi_1^2 \int_0^t \rho^2 dt) - 2k_{lI} \xi_1^2 \int_0^t \rho^2 dt)$  and  $\eta_{lI} = k_{lI} (\rho x - 2\xi_2 \xi_1^2 \int_0^t \rho^2 dt) - (k_{lR}^2 - k_{lI}^2 - 2|c_1|^2) \xi_1^2 \int_0^t \rho^2 dt$ , where  $\tilde{\theta} = -\frac{\rho}{2\rho} x^2 + 2\xi_2 \xi_1^2 (\rho x - \xi_2 \xi_1^2 \int_0^t \rho^2 dt)$ , and all other quantities are given in Appendix B [cf. (B.6)-(B.13)]. Here,  $A_j^{l-}$  ( $A_j^{l+}$ ) is the amplitude of the soliton  $S_l$  in the  $j$ th component,  $l, j = 1, 2$ , before (after) collision, in the absence of Rabi-term and the inhomogeneity, which are defined in Appendix C.1. We notice that in the absence of Rabi term ( $\sigma = 0$ ), there is no oscillatory terms as expected. By computing the densities ( $|\psi_j^{l\pm}|^2$ ,  $j, l = 1, 2$ ) before and after collision and noticing  $|\psi_j^{l+}|^2 = |\psi_j^{l-}|^2$  (since  $|A_j^{l+}| = |A_j^{l-}|$ , see Eqs. (C.1)-(C.4)), we identify that the nature of collision is elastic except for a phase-shift. This phase-shift is same for both solitons  $S_1$  and  $S_2$  that can be found as  $\frac{R_3 - R_2 - R_1}{2}$ . There will be oscillations in bright-dark solitons and also in the background along with a modulation due to nonlinearity and Rabi term.

#### (ii) Collision dynamics in the presence of periodically modulated nonlinearity

The collision of two solitons in the two-component GPEs with periodically modulated nonlinearity  $\rho(t)$  in the absence and presence of Rabi coupling are depicted in Figs. 12 and 13 respectively. For this case the strength of the parabolic trap is given by Eq. (7b).

The role of time modulated scattering length is to introduce periodic modulations in the soliton profile before and after collision uniformly. Meanwhile, the Rabi term leads to

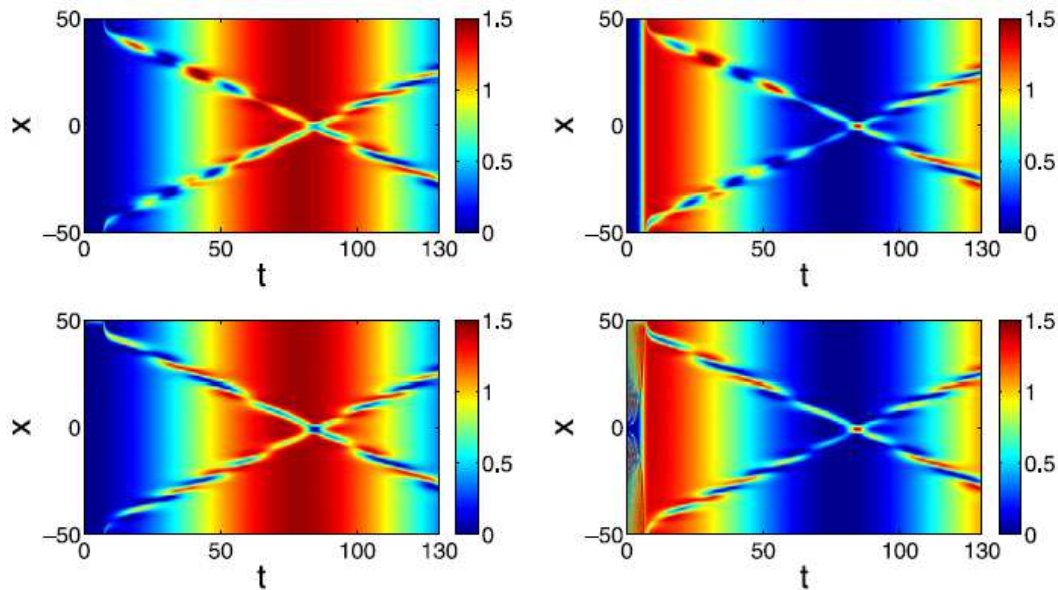


**Figure 11.** Interaction of non-autonomous solitons in two-component GPEs for the kink-like nonlinearity in the presence of Rabi term. Top panels show analytical results (upper left panel:  $\psi_1$  component and right upper panel:  $\psi_2$  component) and bottom panels show numerical results (left bottom panel:  $\psi_1$  component, and right bottom panel:  $\psi_2$  component). The soliton parameters are  $k_1 = -1 + i$ ,  $k_2 = 1 - i$ ,  $c_1 = 3$ ,  $b_1 = 0.2$ ,  $\alpha_1^{(1)} = \alpha_2^{(1)} = 0.03$ ,  $\delta = -4.5$ ,  $\xi_1 = 0.2$ ,  $\xi_2 = 0$ ,  $\omega = 0.75$  and  $\sigma = 0.02$ .

a periodic exchange of condensates between the components along with oscillations in the background. As in the previous example, here also the Rabi coupling makes it feasible to have both dark and bright parts of the mixed soliton in first and second components. We find that the solitons exhibit elastic collision even in the presence of Rabi coupling, though there is an exchange of atoms between the components. This example shows that the Rabi coupling does not affect the elastic nature of the collision in the two-component GPEs. An asymptotic analysis similar to that of kink-like nonlinearity can be carried out for this case too.

### 3. Non-autonomous BD soliton in three-component BECs and Rabi oscillations

Following our considerations for the binary BEC case, we now proceed with the investigation of the three-component system. The dynamics of three-component BECs in 1D with equal time-dependent interaction strengths (i.e.,  $g_{jl} = \rho(t)$ ,  $j, l = 1, 2, 3$ ), and in the presence of external time-dependent harmonic potential  $V_j(x, t) (\equiv V)$ , is governed by the following dimensionless non-autonomous three-coupled GPEs (see, e.g., [3]):

$$i\psi_{j,t} = -\frac{1}{2}\psi_{j,xx} + \rho(t) \sum_{l=1}^3 |\psi_l|^2 \psi_j + \sum_{l=1, (l \neq j)}^3 \sigma_l \psi_l + V(x, t) \psi_j, \quad j = 1, 2, 3, \quad (12)$$

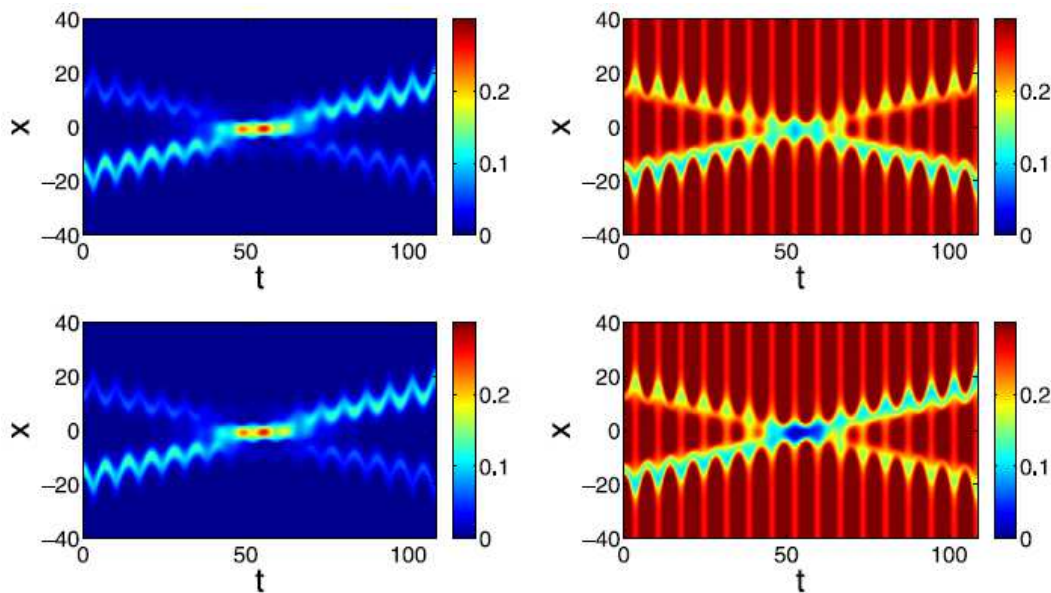


**Figure 12.** Interaction of non-autonomous solitons in two-component GPEs for the periodically modulated nonlinearity in the absence of Rabi term. Top panels show the exact analytical results (upper left panel: bright component and right upper panel: dark component) and bottom panels show numerical results (left bottom panel: bright component and right bottom panel: dark component). The parameter values are chosen as  $k_1 = -1 + i$ ,  $k_2 = 1 - i$ ,  $b_1 = 0.2$ ,  $c_1 = 2$ ,  $\alpha_1^{(1)} = \alpha_2^{(1)} = 0.02$ ,  $\delta = 0$ ,  $\xi_1 = 0.2$ ,  $\xi_2 = 0$ ,  $\varepsilon = 0.2$  and  $\omega = 0.9$ .

where  $\psi_j(x, t)$  are the wave functions of the condensates. As before, coefficients  $\sigma_l$  account for the (linear) Rabi coupling and are chosen to be equal (i.e.,  $\sigma_l \equiv \sigma$ ,  $l=1,2,3$ ); furthermore, the strength of the nonlinear coupling is given by  $\rho(t)$ .

As in the two-component case, we employ a rotation transformation and a similarity transformation (see details in Appendix A) and reduce Eq. (12) in the form:

$$iq_{j,T} + q_{j,XX} - 2 \sum_{l=1}^3 |q_l|^2 q_j = 0, \quad j = 1, 2, 3. \quad (13)$$

The above model, three-coupled NLS system (13), is also a completely integrable system (the three-component generalization of Manakov system with defocusing nonlinearity) and the soliton solutions can be obtained by various methods, e.g., the Inverse Scattering Transform method, the Hirota's direct method, the Bäcklund transformation method, etc.

### 3.1. Non-autonomous mixed (bright-bright-dark) one-soliton solution

The explicit form of the mixed one-soliton solution of Eq. (13), in the form of a bright-bright-dark soliton, can be obtained by means of the Hirota's method [40, 41]. Here, we consider a mixed soliton solution, with the bright part appearing in  $q_1$  and  $q_2$  components, and with the dark part in  $q_3$  component. The exact analytical form of

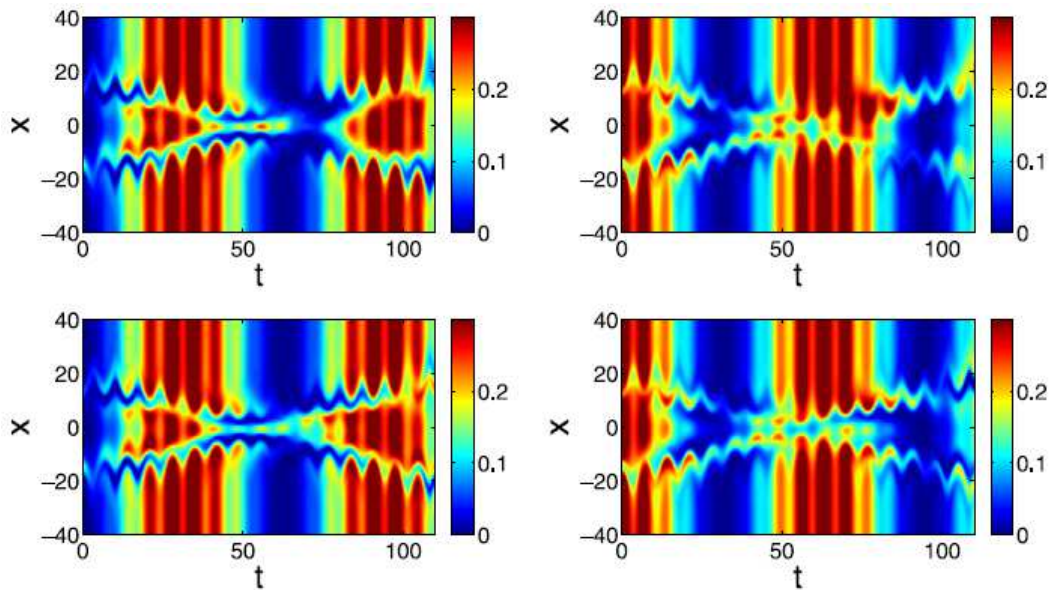


**Figure 13.** Interaction of non-autonomous solitons in two-component GPEs for the periodically modulated nonlinearity in presence of Rabi term. Top panels show the exact analytical results (upper left panel:  $\psi_1$  component, and right upper panel:  $\psi_2$  component). Bottom panels show numerical results (left bottom panel:  $\psi_1$  component and right bottom panel:  $\psi_2$  component). The parameters are  $k_1 = -1 + i$ ,  $k_2 = 1 - i$ ,  $b_1 = 0.2$ ,  $c_1 = 2$ ,  $\alpha_1^{(1)} = \alpha_2^{(1)} = 0.02$ ,  $\delta = 0$ ,  $\xi_1 = 0.2$ ,  $\xi_2 = 0$ ,  $\omega = 0.9$ ,  $\varepsilon = 0.2$  and  $\sigma = 0.05$ .

this type of mixed one- and two-solitons are given in Appendix B.2. Then we make use of the transformations, corresponding to three-component case given in Appendix. A, for obtaining the exact non-autonomous soliton solutions of (12), as in the two-component GPE system.

We again consider the same two forms for  $\rho(t)$  which were discussed in the previous section during our analysis of two-component condensates.

#### (a) Kink-like nonlinearity

Figure 14 shows the mixed one soliton solution of the non-autonomous three-component GPEs. (12) with kink-like nonlinearity. In this case, the shape of the soliton is affected significantly by increasing the value of  $\omega$  as in the two-component case.

Also, we notice that the oscillations of the background are rapid as compared to that of two component case, even for the same value of Rabi coupling  $\sigma$ . This can be inferred by comparing the bottom panels of Fig. 14 and Fig. 3. Thus, an increase in the number of components can make the exchange of atoms between soliton and its background is too faster.

#### (b) Periodically modulated nonlinearity

The propagation of three-component non-autonomous mixed one-soliton in the presence



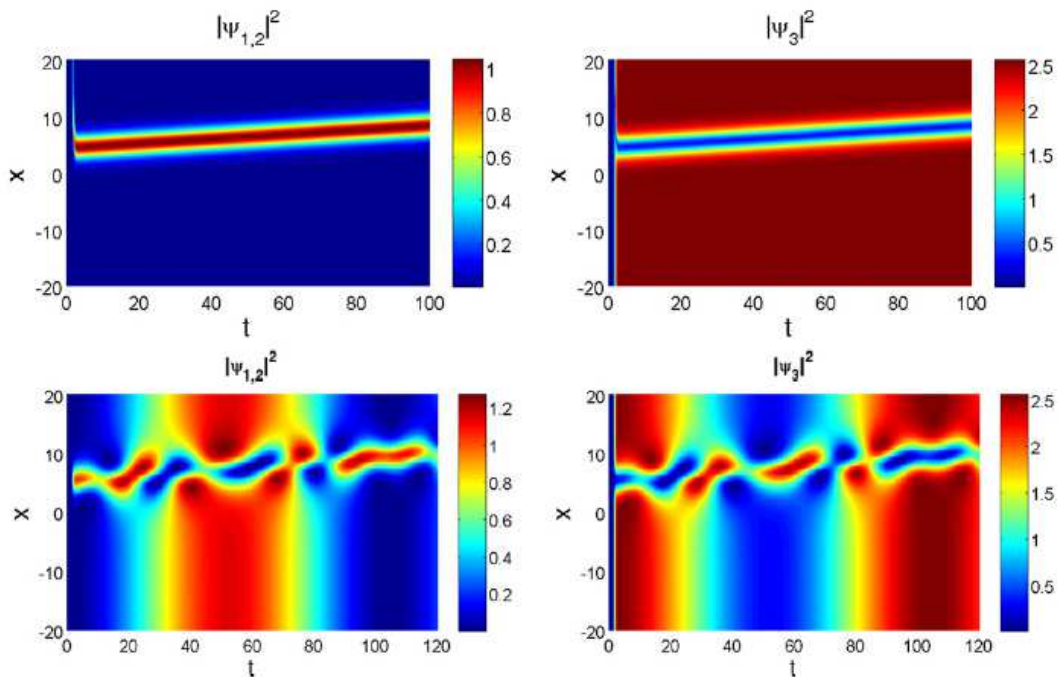


**Figure 14.** Intensity plot of the exact three-component non-autonomous mixed one-soliton solution of Eq. (12) for the kink-like nonlinearity. Top and bottom panels show mixed non-autonomous one soliton in the absence and in the presence of Rabi coupling, respectively. The parameters are  $k_1 = 0.5 + 0.02i$ ,  $b_1 = 0.2$ ,  $\alpha_1^{(1)} = 0.2$ ,  $\alpha_1^{(2)} = 0.2$ ,  $c_1 = 2$ ,  $\delta = -5$ ,  $\xi_1 = 0.4$ ,  $\xi_2 = 0$ ,  $\omega = 2.5$  and  $\sigma = 0.02$ .

of periodically modulated nonlinearity having the form of Mathieu function [see Eq. (7a)] is shown in figure 15. As in the two component case, here also occurs oscillatory transfer of atoms among the components accompanied by oscillations of the background due to Rabi coupling.

The above two examples show that the role of Rabi coupling on three-component non-autonomous BECs is similar to that of two-component BECs except for an increase in the oscillations due to the additional component. Apart from this, we would like to give emphasis to a particular dynamical feature of the three-component system, in the presence of Rabi coupling, which is not possible in the two-component case. It can be recalled from the study on two-component non-autonomous case that it is impossible to make any component (bright/dark) of the mixed soliton to vanish completely, in the presence —as well as in the absence— of Rabi coupling. Contrary, in the three-component system, it is possible to make any one of the bright parts of the mixed soliton to vanish completely before the introduction of Rabi coupling term. The additional component brings an additional arbitrariness to the non-autonomous GPE system (12), which allows to make the density of any one of the bright parts of the mixed soliton to be zero before the incorporation of the Rabi term. The role of the Rabi term is to switch the condensates between all three-components. So, in the presence of Rabi term, some amount of field will be transformed to the component where there was no

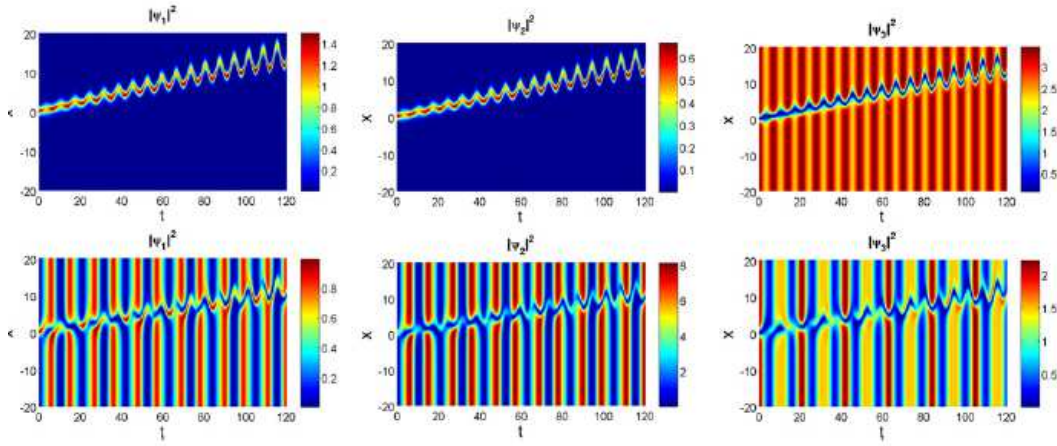


**Figure 15.** Exact three component one-soliton solution of Eq. (10) for the periodically modulated nonlinearity in the absence (top panels,  $\psi_1$ ,  $\psi_2$  and  $\psi_3$  components) and in the presence of Rabi switch (bottom panels,  $\psi_1$ ,  $\psi_2$  and  $\psi_3$  components). The parameters are chosen as  $k_1 = 0.7 + 0.1i$ ,  $b_1 = 0.2$ ,  $\alpha_1^{(1)} = 1.5$ ,  $\alpha_1^{(2)} = 1$ ,  $c_1 = 1$ ,  $\xi_1 = 1$ ,  $\xi_2 = 0$ ,  $\omega = 0.9$ ,  $\delta = 0$ ,  $\varepsilon = 0.2$  and  $\sigma = 0.2$ .

field before its introduction. Thus, in three-component condensates one can transfer a significant part of the condensates to a component which admits no field at all before the introduction of Rabi coupling from the other components. This is shown in Figs. 16 and 17, in which the condensate is completely absent in the second component in Fig. 16 but, after introducing the Rabi coupling, appreciable portion of condensate appears in the same component as shown in Fig. 17.

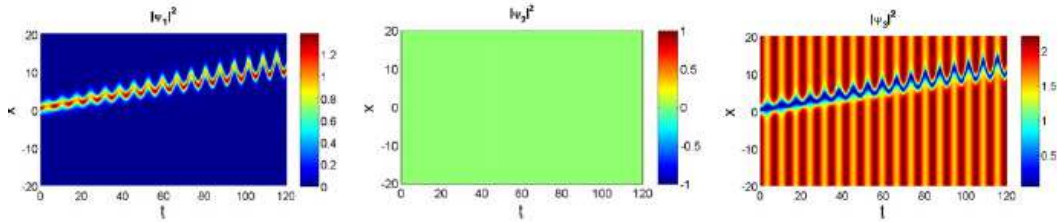


**Figure 16.** Three-component one-soliton solution with periodically modulated nonlinearity in the absence of Rabi coupling. The parameters are  $k_1 = 0.5 + 0.1i$ ,  $b_1 = 0.2$ ,  $\alpha_1^{(1)} = 1$ ,  $\alpha_1^{(2)} = 0$ ,  $\xi_1 = 1$ ,  $c_1 = 1$ ,  $\xi_2 = 0$ ,  $\varepsilon = 0.2$  and  $\omega = 0.8$ .

### 3.2. Non-autonomous mixed (bright-bright-dark) two-soliton collision

The explicit form of mixed two-soliton solution of (13) with the bright parts appearing in components  $(q_1, q_2)$  and the dark part in  $q_3$ , obtained by Hirota's bilinearization method is given in Appendix B.2 and the corresponding asymptotic analysis is presented in Appendix C.2.

From the asymptotic expressions (C.5) and (C.7) one can find that the amplitudes

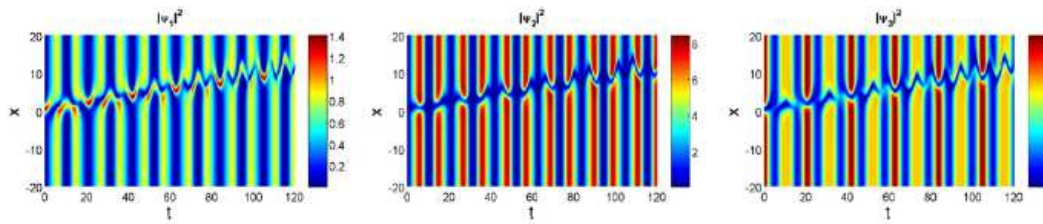


**Figure 17.** Three-component one-soliton solution with periodically modulated nonlinearity in the presence of Rabi coupling. The parameters are  $k_1 = 0.5 + 0.1i$ ,  $b_1 = 0.2$ ,  $\alpha_1^{(1)} = 1$ ,  $\alpha_1^{(2)} = 0$ ,  $c_1 = 1$ ,  $\xi_1 = 1$ ,  $\xi_2 = 0$ ,  $\varepsilon = 0.2$ ,  $\omega = 0.8$  and  $\sigma = 0.2$ .

(condensate densities) of the colliding solitons before and after collision can be related

$$|A_j^{l+}|^2 = |T_j^l|^2 |A_j^{l-}|^2, \quad j, l = 1, 2,$$

where  $|T_j^1|^2 = \frac{e^{2\delta_{2j} - (R_3 + R_2 - R_1)}}{|\alpha_1^{(j)}|^2}$  and  $|T_j^2|^2 = \frac{e^{2\delta_{1j} - (R_1 + R_3 - R_2)}}{|\alpha_2^{(j)}|^2}$ ,  $j = 1, 2$ , where  $\delta_{1j}$ ,  $\delta_{2j}$ ,  $R_1$ ,  $R_2$  and  $R_3$  are defined in Appendix B.2. It is instructive to notice that  $|T_j^l|$ ,  $j, l = 1, 2$ , are not unimodular, in general, and also depend on dark soliton parameters  $c_1$  and  $b_1$  in addition to the bright soliton parameters. This will result in the energy sharing collision displaying suppression (enhancement) of condensate density in the bright part of a given soliton with commensurate changes in the bright part of the other colliding soliton. However, one can have standard elastic collision for the choice  $\frac{\alpha_1^{(1)}}{\alpha_1^{(2)}} = \frac{\alpha_2^{(1)}}{\alpha_2^{(2)}}$ , for which  $|T_j^l|$ ,  $j, l = 1, 2$ , become unimodular. Additionally, the colliding solitons also experience a phase-shift  $\Phi_1 = \Phi_2 = \frac{(R_3 - R_2 - R_1)}{2}$ .

It can also be inferred from the asymptotic expressions (C.6) and (C.8) that the dark solitons in the  $q_3$  component always exhibit elastic collision as  $|A_3^{l-}|^2 = |A_3^{l+}|^2$ ,  $l = 1, 2$ . These dark solitons also undergo a phase-shift, same as that of bright solitons.

This study can be straightforwardly extended to integrable  $N$ -component CNLS system with defocusing nonlinearity, for  $N > 3$ . It is interesting to note that the above kind of energy sharing collision in such  $N$ -component CNLS system can take place only if the bright part of the mixed soliton appears at least in two-components.

Such fascinating energy sharing collision in the three-component GPE system (13), is shown in Fig. 18. In Fig. 18, the bright part of the mixed soliton  $S_1$  is enhanced in the  $q_1$  component whereas it is suppressed in the  $q_2$  component after its collision with the soliton  $S_2$ . The reverse scenario takes place for the bright parts of the mixed soliton  $S_2$ . Notice that the dark parts of mixed solitons  $S_1$  and  $S_2$  are unaffected by the collision. The energy sharing collision is characterized by an exchange of condensates among the bright parts of the colliding mixed solitons  $S_1$  and  $S_2$ , leaving the dark part unaltered after collision. This type of energy sharing collision in different integrable CNLS systems appearing in nonlinear optics has been extensively studied in references [28, 29, 39, 40].

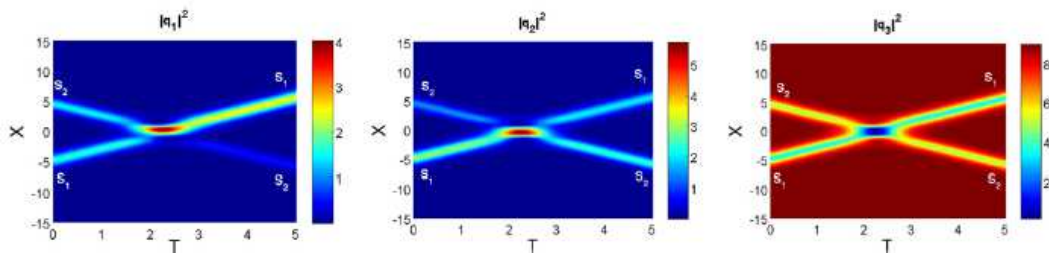


**Figure 18.** Energy sharing collision of mixed solitons in the three-component CNLS equations (see Eq. (13)). The parameters are  $k_1 = -1 + i$ ,  $k_2 = 1.1 - i$ ,  $b_1 = 0.2$ ,  $c_1 = 3$ ,  $\alpha_1^{(1)} = 0.02$ ,  $\alpha_2^{(1)} = 0.01 + 0.025i$  and  $\alpha_1^{(2)} = \alpha_2^{(2)} = 0.02$ .

The non-autonomous two-soliton solution can be expressed as

$$\psi_j = \frac{1}{3}\xi_1\sqrt{2\rho}e^{i\tilde{\theta}} \left[ e^{-2i\sigma t} \sum_{l=1}^3 q_l + e^{i\sigma t} \left( 2q_j - \sum_{l=1, l \neq j}^3 q_l \right) \right], \quad j = 1, 2, 3, \quad (14)$$

where  $q_j$  are given in Eqs. (B.18-B.19) in which  $X$  and  $T$  are defined by equations (A.6) and (A.7), respectively. Now, it is of further interest to study whether the above discussed energy sharing collision still prevails in the presence of time-varying nonlinearity and Rabi coupling. For illustrative purpose, again we consider the two types of the time-dependent nonlinearities discussed in the two-component case.

(i) *Energy sharing collision of mixed solitons in non-autonomous three-component GPE.*

### (a) Kink-like nonlinearity

The soliton collision for a kink-like modulated nonlinearity in the context of the non-autonomous three-component GPEs. (12), in the presence of Rabi term, is depicted in Fig. 19. The density of the bright part of the mixed soliton  $S_1$  gets enhanced and  $S_2$  is suppressed after the collision in the  $\psi_1$  component, whereas the component  $\psi_2$  experiences reverse effects for  $S_1$  and  $S_2$ , and the dark parts of mixed solitons in  $\psi_3$  component remain unaltered. Thus, the switching nature of energy sharing collision in the autonomous system (13) is unaffected by the presence of Rabi term in the non-autonomous GP system, for this choice of time-dependent nonlinearity and external potential. This shows that the energy sharing collision of bright parts of the mixed solitons can exist for a wide range of time-dependence of nonlinearity, external potential and Rabi coupling, for which the non-autonomous system (12) is integrable. An asymptotic analysis of the non-autonomous two-soliton solution (14) can be carried out as in the two-component case. One can notice that the energy sharing collision still prevails as  $|A_j^{l+}| \neq |A_j^{l-}|$ ,  $j, l = 1, 2$ , in general, which ultimately leads to  $|\psi_j^{l+}| \neq |\psi_j^{l-}|$ . The phase-shift can be found to be the same for both the solitons and is given by  $\frac{(R_3 - R_2 - R_1)}{2}$ , where  $R_1$ ,  $R_2$  and  $R_3$  are defined in Appendix B.

In the two-component case, we observe a gradual increase in the density of

condensates in the bright parts in the region  $t = 2$  to  $6$  and it remains constant for  $t > 6$ , due to the nature of nonlinearity (Fig. 10) and onset of Rabi oscillations due to Rabi coupling (see Fig. 11). Note that, there the collision is elastic in the absence as well as in the presence of Rabi coupling and is not an energy sharing one. Thus, in two-component BECs the growth of condensate is purely due to the nature of  $\rho(t)$ . However, in the present case, for the mixed soliton  $S_2$  there is a suppression in the

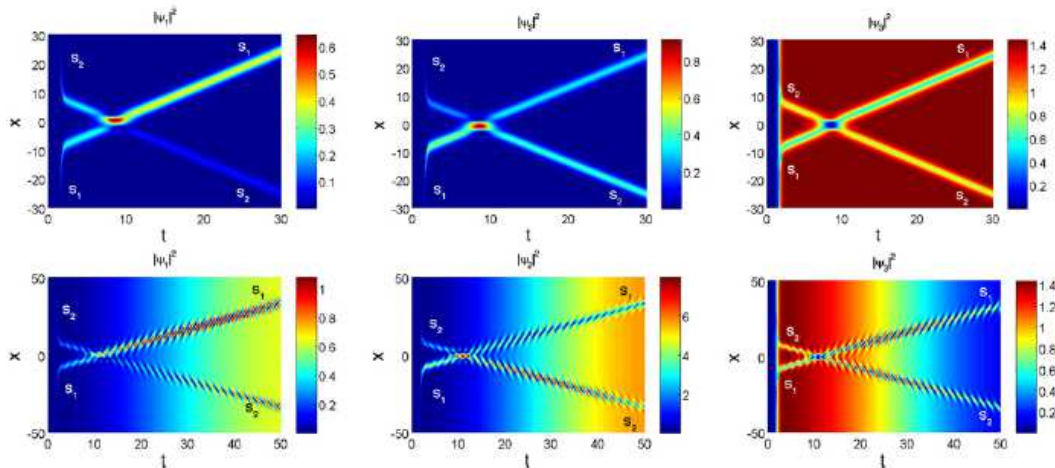


**Figure 19.** Energy sharing collision of mixed solitons in the non-autonomous three-component GP Eq. (12) with kink like nonlinearity in the absence (top panels) and in the presence (bottom panel) of Rabi coupling. The soliton parameters are  $k_1 = -1 + i$ ,  $k_2 = 1.1 - i$ ,  $b_1 = 0.2$ ,  $c_1 = 3$ ,  $\alpha_1^{(1)} = 0.02$ ,  $\alpha_2^{(1)} = 0.01 + 0.025i$ ,  $\alpha_1^{(2)} = \alpha_2^{(2)} = 0.02$ ,  $\xi_1 = 0.2$ ,  $\xi_2 = 0$ ,  $\delta = -4$ ,  $\omega = 2$  and  $\sigma = 0.02$ .

density of its bright part in  $\psi_1$  after interaction due to the energy sharing collision. This suppression balances the enhancement in its density in this regime due to the nature of the time-varying nonlinearity, and will result in standard soliton ( $S_2$ ) with constant amplitude after interaction (see Fig. 19). Also, the Rabi term leads to beating effects in this soliton  $S_2$  in  $\psi_1$ , but with a smaller period as compared to that of the two-component case. However, the opposite effect takes place for  $S_2$  in the second component  $\psi_2$ . This shows that energy sharing collision can be profitably used in altering the exchange of condensates through Rabi switching.

### (b) Periodic modulated nonlinearity

Energy sharing collision of mixed solitons in the three-component GPEs with periodically modulated nonlinearity is shown in Fig. 20. We observe that in this case also the energy sharing collision for the non-autonomous system (1) takes place as that of the autonomous system (2) (see Fig. 18).

We observe another dramatic switching of condensates during collision of two solitons in the non-autonomous three-component GPEs. (12) with periodically modulated time-dependent nonlinearity, for smaller values of Rabi term  $\sigma$ . Here,

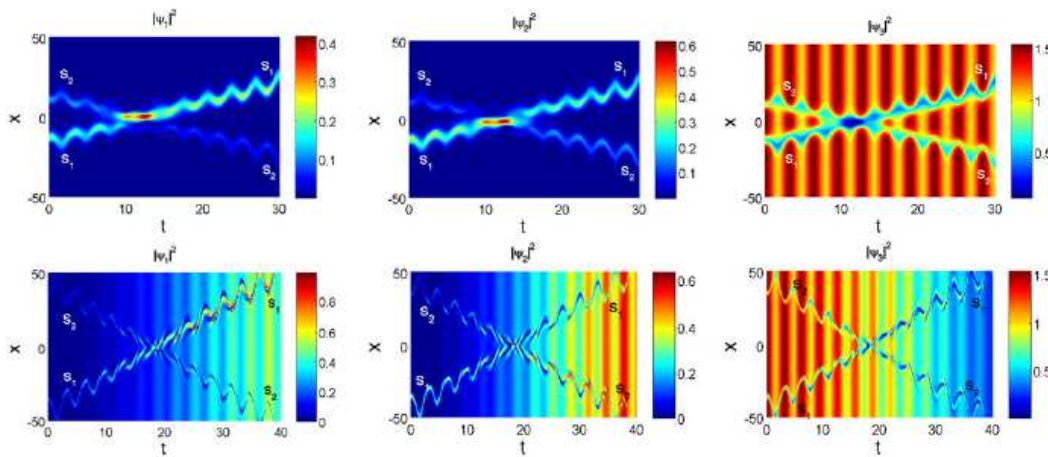


**Figure 20.** Energy sharing collision of mixed soliton in the non-autonomous three-component GPEs with periodically modulated nonlinearity in the absence (top panels) and in the presence (bottom panels) of Rabi coupling. The choice of soliton parameters are  $k_1 = -1 + i$ ,  $k_2 = 1 - i$ ,  $b_1 = 0.2$ ,  $c_1 = 2$ ,  $\alpha_1^{(1)} = 0.02$ ,  $\alpha_2^{(1)} = 0.01 + 0.025i$ ,  $\alpha_1^{(2)} = \alpha_2^{(2)} = 0.02$ ,  $\delta = 0$ ,  $\xi_1 = 0.4$ ,  $\xi_2 = 0$ ,  $\omega = 2$ ,  $\varepsilon = 0.2$  and  $\sigma = 0.02$ .

before collision, we have an oscillating bright soliton part ( $S_2$ ) in the  $\psi_1$  component, which completely transforms to an oscillating mixed (bright-dark) soliton in the same component after collision. In the second component,  $\psi_2$ , the amplitude of bright soliton part ( $S_2$ ) gets enhanced after the collision. For the soliton  $S_1$ , in  $\psi_1$  ( $\psi_2$ ) component enhancement (suppression) with periodic oscillations takes place. In the component  $\psi_3$  the solitons undergo elastic collision and there occurs only switching of condensates due to Rabi coupling. Notably, in  $\psi_3$  component the pure bright part of  $S_1$  is transformed to mixed (BD) part after collision (see  $\psi_3$  component in the bottom panel of Fig. 20). This interesting collision is a consequence of the combined effects of time-dependent nonlinearity and external potential, Rabi term and the exchange of condensates due to energy sharing collision. Another noticeable effect arising due to the Rabi coupling, particularly for this type of periodic nonlinearity, is an increase in the relative separation distance between the solitons well before and after collision. Furthermore, the collision takes place faster in the presence of Rabi term.

#### 4. Conclusions

In this work, we have studied the dynamics of non-autonomous mixed bright-dark matter-wave solitons in two- and three-component Bose-Einstein condensates. Our setting included a time-dependent parabolic potential and scattering length, as well as Rabi coupling between separate hyperfine states. We have transformed the non-autonomous two- and three-component Gross-Pitaevskii equations, into a set of integrable defocusing two- and three-component Manakov autonomous systems by means of two successive transformations. These transformations can be viewed as a

rotation followed by a similarity transformation. Then, with the aid of the two- and three-component soliton solutions of defocusing Manakov systems, and by inverting the transformations, we have studied the dynamics of single- and multiple-non-autonomous matter-wave solitons. Our considerations involved two different choices of nonlinearities namely, a kink-like and Mathieu-like ones, together with their corresponding time-varying harmonic potentials.

Our study on the two-component case has shown that the nature of soliton propagation depends significantly on the nature of nonlinearity and the associated potential. The switching depends purely on the Rabi coupling. Here, the bright-dark matter-wave solitons exhibit elastic collisions along with oscillations due to Rabi coupling, and profile modulation due to the nonlinearity  $\rho(t)$  and strength of the potential. In this two-component non-autonomous case, the dark-bright solitons exist as “symbiotic” structures, i.e., the bright component exist only due to the presence of its dark counterpart. Hence it is impossible to make any part (either bright or dark) to be zero. Also, Rabi coupling makes it possible to have a special type of mixed soliton in which bright and dark parts can co-exist in the same component. Such structures are reminiscent to the so-called beating dark-dark solitons, which have recently been observed in autonomous binary BECs [14,42]. The present study shows the possibility of observing such structures, with co-existing bright and dark parts in the same component, also in non-autonomous multi-component systems in the presence of Rabi coupling. Our analytical results of the two-component non-autonomous GPE system are found to be in very good agreement with results of direct numerical simulations.

We have also studied non-autonomous three-component BECs. An important observation in this case is that the bright part of the mixed soliton can be absent in any of the three-component condensate in the absence of Rabi coupling. The introduction of Rabi coupling makes it feasible to have some portion of mixed-soliton in that component. Also, in the three-component BECs the number of oscillations increases as compared to that of two-component case and ultimately the exchange of atoms between the soliton and background also increases in a periodic manner.

Finally, we considered the collision of non-autonomous solitons in the three-component condensate. In this case, the non-autonomous matter-wave solitons undergo interesting energy-sharing collision, leading to an exchange of atoms, in addition to Rabi coupling, in the bright ( $\psi_1$  and  $\psi_2$ ) components; notice that in the third component ( $\psi_3$ ) the solitons undergo elastic collision. The matter-wave mixed (bright-bright-dark) soliton collision in non-autonomous three-component condensates also displays another fascinating feature, namely the reversal of the type of mixed- soliton part (i.e., bright type to dark type or vice-versa).

Our study can be extended to other types of forms for nonlinearity modulation by identifying the corresponding modulation of the harmonic potential using the Riccati Eq. (A.8) and vice-versa. The agreement between the numerical and analytical results indicates that the presented exact non-autonomous solution can well be utilised for the purpose of studying non-integrable multi- component GPE type systems with Rabi

coupling. It is of future interest to investigate the effect of spatial and spatio-temporal modulations of nonlinearity. Works along these directions are in progress. This study may have ramifications in the design of matter-wave devices (e.g., switches) and also in experiments involving growth and oscillations of condensates.

## Acknowledgments

The work of T.K. is supported by Department of Science and Technology (DST), Government of India, in the form of a major research project. R.B.M. acknowledges the financial support from DST in the form of Project Assistant. T.K. and R.B.M. also thank the principal and management of Bishop Heber College for constant support and encouragement. The work of F.T., H.E.N., and D.J.F. was partially supported by the Special Account for Research Grants of the University of Athens.

## Appendix A. Mapping non-autonomous GPEs to integrable CNLS systems

In this Appendix, we explicitly show that the non-autonomous two- and three-component GP systems [cf. Eqs. (1) and (12)] with Rabi coupling can be transformed to integrable CNLS systems, i.e., the Manakov model and its three component generalization, with defocusing nonlinearities; this will be done by means of two successive transformations. In particular, in the case of the two-component BEC, first we apply the following unitary transformation to Eq. (1) with  $g_{jl} = \rho(t)$  and  $\sigma_1 = \sigma_2 = \sigma$ :

$$\begin{pmatrix} \psi_1 \\ \psi_2 \end{pmatrix} = \begin{pmatrix} \cos(\sigma t) & -i\sin(\sigma t) \\ -i\sin(\sigma t) & \cos(\sigma t) \end{pmatrix} \begin{pmatrix} \phi_1 \\ \phi_2 \end{pmatrix}. \quad (\text{A.1})$$

In the case of the three-component BECs, a similar transformation is applied to Eq. (12); this transformation is of the form [30, 32]:

$$\begin{pmatrix} \psi_1 \\ \psi_2 \\ \psi_3 \end{pmatrix} = \frac{1}{3} \begin{pmatrix} (2e^{i\sigma t} + e^{-2i\sigma t}) & (e^{-2i\sigma t} - e^{i\sigma t}) & (e^{-2i\sigma t} - e^{i\sigma t}) \\ (e^{-2i\sigma t} - e^{i\sigma t}) & (2e^{i\sigma t} + e^{-2i\sigma t}) & (e^{-2i\sigma t} - e^{i\sigma t}) \\ (e^{-2i\sigma t} - e^{i\sigma t}) & (e^{-2i\sigma t} - e^{i\sigma t}) & (2e^{i\sigma t} + e^{-2i\sigma t}) \end{pmatrix} \begin{pmatrix} \phi_1 \\ \phi_2 \\ \phi_3 \end{pmatrix}. \quad (\text{A.2})$$

This way, we obtain the following set of non-autonomous equations without the Rabi coupling term:

$$i\phi_{j,t} = -\frac{1}{2}\phi_{j,xx} + \left( \rho(t) \sum_{l=1}^N |\phi_l|^2 + V(x, t) \right) \phi_j, \quad (\text{A.3})$$

where  $N = 2$  and  $j = 1, 2$ , for Eq. (1), while  $N = 3$  and  $j = 1, 2, 3$  for Eq. (12). Then, by performing the similarity transformation

$$\phi_j(x, t) = \xi_1 \sqrt{2\rho(t)} e^{i\tilde{\theta}} q_j(X, T), \quad (\text{A.4})$$



where

$$\tilde{\theta} = -\frac{1}{2} \left[ \frac{d}{dt} (\ln \rho) \right] x^2 + 2\xi_2 \xi_1^2 \left( \rho x - \xi_2 \xi_1^2 \int_0^t \rho^2 dt \right), \quad (\text{A.5})$$

$$X = \sqrt{2} \xi_1 \left( \rho x - 2\xi_2 \xi_1^2 \int_0^t \rho^2 dt \right), \quad (\text{A.6})$$

$$T = \xi_1^2 \int_0^t \rho^2 dt, \quad (\text{A.7})$$

with  $\xi_1$  and  $\xi_2$  being arbitrary real constants, Eq. (A.3) can be transformed into the system of Eq. (2) for the two-component system, or to Eq. (13) for the three-component system, with the condition

$$\frac{d\Lambda}{dt} - \Lambda^2 - \Omega^2(t) = 0, \quad (\text{A.8})$$

where  $\Lambda = (\rho_t/\rho)$ . Equation (A.8) is nothing but a Riccati-type equation. Notice that similar type of transformation has been reported for two-component BECs [26] but in the absence of Rabi coupling.

## Appendix B. One- and two-soliton solutions of the integrable two- and three- component defocusing CNLS systems

### Appendix B.1. Bright-dark solitons in the two-component system (2)

The bright-dark one-soliton solution of Eq. (2), with bright (dark) part appearing in the  $q_1$  ( $q_2$ ) component, obtained by Hirota's bilinearization method [27, 39].

$$q_1(X, T) = \sqrt{|c_1|^2 \cos^2 \varphi_1 - k_{1R}^2} \operatorname{sech}[k_{1R}(X - 2k_{1I}T) + R/2] e^{i(\eta_{1I} + \theta)}, \quad (\text{B.1})$$

$$q_2(X, T) = -c_1 e^{i(\zeta_1 + \varphi_1)} (\cos \varphi_1 \tanh[k_{1R}(X - 2k_{1I}T) + R/2] + i \sin \varphi_1), \quad (\text{B.2})$$

where  $\varphi_1 = \tan^{-1}(\frac{k_{1I} - b_1}{k_{1R}})$ ,  $\zeta_1 = -(b_1^2 + 2|c_1|^2)T + b_1X$ ,  $\alpha_1^{(1)} = \alpha_{1R}^{(1)} + i\alpha_{1I}^{(1)}$ ,  $\theta = \tan^{-1}(\frac{\alpha_{1I}}{\alpha_{1R}})$ ,  $\eta_1 = k_1X + i(k_1^2 - 2|c_1|^2)T$  and  $e^R = -\frac{1}{(k_1 + k_1^*)^2} \left( 1 - \frac{|c_1|^2}{|k_1 - ib_1|^2} \right)^{-1}$ . The bright part of the mixed soliton is characterized by three complex parameters  $k_1$ ,  $\alpha_1$ , and  $c_1$ , and one real parameter  $b_1$ . Note that  $\alpha_1$  does not affect the amplitude of the soliton. The dark soliton part of the mixed soliton also influences the bright part through the parameters  $c_1$  and  $b_1$ . Also, the solution becomes non-singular only for the choice  $|c_1|^2 > |k_1 - ib_1|^2$ . As a consequence of this, it is impossible to make either one of the soliton part (i.e., dark/bright) completely zero. Thus, the bright and the dark parts of the mixed soliton co-exist but appear in separate components due to the presence of the other and can be viewed as ‘‘symbiotic solitons’’, as mentioned in the introduction.

On the other hand, the explicit form of mixed two-soliton solution of the integrable 2-CNLS system (2) can be written as [27]:

$$q_1(X, T) = \frac{1}{D} \left( \alpha_1^{(1)} e^{\eta_1} + \alpha_2^{(1)} e^{\eta_2} + e^{\eta_1 + \eta_1^* + \eta_2 + \delta_{11}} + e^{\eta_2 + \eta_2^* + \eta_1 + \delta_{21}} \right), \quad (\text{B.3})$$

$$q_2(X, T) = \frac{c_1 e^{i\zeta_1}}{D} \left[ 1 + e^{\eta_1 + \eta_1^* + Q_{11}} + e^{\eta_1 + \eta_2^* + Q_{12}} + e^{\eta_2 + \eta_1^* + Q_{21}} + e^{\eta_2 + \eta_2^* + Q_{22}} + e^{\eta_1 + \eta_1^* + \eta_2 + \eta_2^* + Q_3} \right], \quad (\text{B.4})$$

where

$$D = 1 + e^{\eta_1 + \eta_1^* + R_1} + e^{\eta_1 + \eta_2^* + \delta_0} + e^{\eta_2 + \eta_1^* + \delta_0^*} + e^{\eta_2 + \eta_2^* + R_2} + e^{\eta_1 + \eta_1^* + \eta_2 + \eta_2^* + R_3}. \quad (\text{B.5})$$

The various parameters in the above equation are defined below:

$$e^{R_1} = \mu_{11}, \quad e^{R_2} = \mu_{22}, \quad e^{\delta_0} = \mu_{12}, \quad e^{\delta_0^*} = \mu_{21}, \quad \zeta_1 = -(b_1^2 + \lambda)T + b_1X, \quad (\text{B.6})$$

$$\eta_j = k_jX + i(k_j^2 - \lambda)T, \quad \lambda = 2|c_1|^2, \quad e^{Q_{ij}} = -\left(\frac{k_i - ib_1}{k_j^* + ib_1}\right) \mu_{ij}, \quad i, j = 1, 2, \quad (\text{B.7})$$

$$e^{Q_3} = -\left(\frac{(k_1 - ib_1)(k_2 - ib_1)}{(k_1^* + ib_1)(k_2^* + ib_1)}\right) e^{R_3}, \quad (\text{B.8})$$

$$e^{R_3} = |k_1 - k_2|^2 \mu_{11} \mu_{12} \mu_{21} \mu_{22} (\chi_{12} \chi_{21} - \chi_{11} \chi_{22}), \quad (\text{B.9})$$

$$\mu_{il} = \frac{1}{(k_i + k_l^*) \chi_{il}}, \quad i, l = 1, 2, \quad (\text{B.10})$$

$$e^{\delta_{11}} = (k_2 - k_1) \mu_{11} \mu_{21} (\alpha_2^{(1)} \chi_{21} - \alpha_1^{(1)} \chi_{11}), \quad (\text{B.11})$$

$$e^{\delta_{21}} = (k_2 - k_1) \mu_{12} \mu_{22} (\alpha_2^{(1)} \chi_{22} - \alpha_1^{(1)} \chi_{12}), \quad (\text{B.12})$$

$$\chi_{il} = -\left[\frac{(k_i + k_l^*)}{(\alpha_i^{(1)} \alpha_l^{(1)*})} \left(1 - \frac{|c_1|^2}{(k_i - ib_1)(k_l^* + ib_1)}\right)\right], \quad i, l = 1, 2. \quad (\text{B.13})$$

### Appendix B.2. Bright-bright-dark solitons in the three-component system (13)

The one-soliton solution of Eq. (13), in the form of a bright-bright-dark soliton, obtained by Hirota's bilinearization method is given below:

$$q_j(X, T) = A_j \sqrt{|c_1|^2 \cos^2 \varphi_1 - k_{1R}^2} \operatorname{sech}[k_{1R}(X - 2k_{1I}T) + R/2] e^{i\eta_{1I}}, \quad j = 1, 2, \quad (\text{B.14})$$

$$q_3(X, T) = -c_1 e^{i(\zeta_1 + \varphi_1)} (\cos \varphi_1 \tanh[k_{1R}(X - 2k_{1I}T) + R/2] + i \sin \varphi_1), \quad (\text{B.15})$$

where

$$\varphi_1 = \tan^{-1} \left( \frac{k_{1I} - b_1}{k_{1R}} \right), \quad A_j = \left( \frac{\alpha_1^{(j)}}{\sqrt{|\alpha_1^{(1)}|^2 + |\alpha_1^{(2)}|^2}} \right), \quad j = 1, 2, \quad (\text{B.16})$$

$$e^R = \frac{\sum_{j=1}^2 (\alpha_1^{(j)} \alpha_1^{(j)*})}{(k_1 + k_1^*)^2} \left( \frac{|c_1|^2}{|k_1 - ib_1|^2} - 1 \right)^{-1}. \quad (\text{B.17})$$

The above soliton solution is characterized by three complex parameters  $c_1$ ,  $\alpha_1^{(1)}$ ,  $\alpha_1^{(2)}$ , and one real parameter  $b_1$  along with the non-singular condition  $|c_1|^2 > |k_1 - ib_1|^2$ . Parameters  $A_j$  may be viewed as spin-polarization in the case of spinor condensates [15, 16].

On the other hand, the respective two-soliton solution of Eq. (13) can be obtained as follows:

$$q_j(X, T) = \frac{1}{D} \left( \alpha_1^{(j)} e^{\eta_1} + \alpha_2^{(j)} e^{\eta_2} + e^{\eta_1 + \eta_1^* + \eta_2 + \delta_{1j}} + e^{\eta_2 + \eta_2^* + \eta_1 + \delta_{2j}} \right), \quad j = 1, 2, \quad (\text{B.18})$$

$$q_3(X, T) = \frac{c_1 e^{i\zeta_1}}{D} \left[ 1 + e^{\eta_1 + \eta_1^* + Q_{11}} + e^{\eta_1 + \eta_2^* + Q_{12}} + e^{\eta_2 + \eta_1^* + Q_{21}} \right. \\ \left. + e^{\eta_2 + \eta_2^* + Q_{22}} + e^{\eta_1 + \eta_1^* + \eta_2 + \eta_2^* + Q_3} \right], \quad (\text{B.19})$$

where

$$D = 1 + e^{\eta_1 + \eta_1^* + R_1} + e^{\eta_1 + \eta_2^* + \delta_0} + e^{\eta_2 + \eta_1^* + \delta_0^*} + e^{\eta_2 + \eta_2^* + R_2} + e^{\eta_1 + \eta_1^* + \eta_2 + \eta_2^* + R_3}. \quad (\text{B.20})$$

The various parameters in the above equation are defined below

$$\zeta_1 = -(b_1^2 + \lambda)T + b_1X, \quad (\text{B.21})$$

$$e^{\delta_{1j}} = (k_2 - k_1)\mu_{11}\mu_{21}(\alpha_2^{(j)}\chi_{21} - \alpha_1^{(j)}\chi_{11}), \quad (\text{B.22})$$

$$e^{\delta_{2j}} = (k_2 - k_1)\mu_{12}\mu_{22}(\alpha_2^{(j)}\chi_{22} - \alpha_1^{(j)}\chi_{12}), \quad j = 1, 2, \quad (\text{B.23})$$

$$\mu_{il} = \frac{1}{(k_i + k_l^*)\chi_{il}}, \quad (\text{B.24})$$

$$\chi_{il} = - \left[ \frac{(k_i + k_l^*)}{\sum_{j=1}^2 (\alpha_i^{(j)} \alpha_l^{(j)*})} \left( 1 - \frac{|c_1|^2}{(k_i - ib_1)(k_l^* + ib_1)} \right) \right], \quad i, l = 1, 2. \quad (\text{B.25})$$

The other parameters  $R_1$ ,  $R_2$ ,  $R_3$ ,  $\delta_0$ , and  $\delta_0^*$  in the above equation are similar to that of the mixed two-soliton solution for the two-component case, given after Eq. (B.5), with the above redefinition of  $\chi_{il}$ .

## Appendix C. Asymptotic analysis

### Appendix C.1. Asymptotic analysis of two-soliton solution of the Manakov system (2)

In this Appendix, we present the asymptotic forms of the two colliding solitons obtained by performing the asymptotic analysis of the two-soliton solution given by Eqs. (B.3)-(B.5). For the analysis, we choose  $k_{1R} < k_{2R}$  and  $k_{1I} > k_{2I}$ , without loss of generality.

#### Before collision

$$q_1^{l-} = A_1^{l-} \operatorname{sech} \left( \eta_{lR} + \frac{R_l}{2} \right) e^{i\eta_{lI}}, \quad (\text{C.1})$$

$$q_2^{l-} = A_2^{l-} \left[ \cos\varphi_l \tanh \left( \eta_{lR} + \frac{R_l}{2} \right) + i \sin\varphi_l \right], \quad l = 1, 2. \quad (\text{C.2})$$

#### After collision

$$q_1^{l+} = A_1^{l+} \operatorname{sech} \left( \eta_{lR} + \frac{R_3 - R_{3-l}}{2} \right) e^{i\eta_{lI}}, \quad (\text{C.3})$$

$$q_2^{l+} = A_2^{l+} \left[ \cos\varphi_l \tanh \left( \eta_{lR} + \frac{R_3 - R_{3-l}}{2} \right) + i \sin\varphi_l \right], \quad l = 1, 2, \quad (\text{C.4})$$

where  $\eta_{lR} = k_{lR}(X - 2k_{lI}T)$ ,  $\eta_{lI} = k_{lI}X - (k_{lR}^2 - k_{lI}^2 - 2|c_1|^2)T$ ,  $A_1^{l-} = \frac{\alpha_l^{(1)}}{2}e^{-R_l/2}$ ,  $A_2^{l-} = -c_1 e^{i(\zeta_1 + \varphi_l)}$ ,  $A_1^{l+} = \frac{1}{2}e^{-(R_{3-l} + R_3)/2 + \delta_{l1}}$  and  $A_2^{l+} = c_1 e^{-i(\zeta_1 + 2\varphi_{3-l} + \varphi_l)}$ . Here and in the following, as mentioned in the text, the superscript (subscript) in  $q$  (or  $\psi$ ) and in  $A$  represents the number of soliton (component) while -(+) appearing in the corresponding quantities indicates their form before (after) collision. All the quantities found in Eqs. (C.1)-(C.4) are defined below Eq. (B.5). From the above expressions it can be easily verified that  $|A_i^{l+}|^2 = |A_i^{l-}|^2$ ,  $i, l = 1, 2$ .

### Appendix C.2. Asymptotic analysis of two-soliton solution of integrable three coupled NLS system (13)

In this Appendix, we present the results of the asymptotic analysis of two-soliton solution of Eq. (13) [see Eqs. (B.18) and (B.19)] briefly. As before, here also without loss of generality, we choose  $k_{1R} < k_{2R}$ ,  $k_{1I} > k_{2I}$ . The asymptotic forms are given below:

#### Before collision

$$q_j^{l-} = A_j^{l-} \operatorname{sech} \left( \eta_{lR} + \frac{R_l}{2} \right) e^{i\eta_{lI}}, \quad (\text{C.5})$$

$$q_3^{l-} = A_3^{l-} \left[ \cos\varphi_l \tanh \left( \eta_{lR} + \frac{R_l}{2} \right) + i \sin\varphi_l \right], \quad j, l = 1, 2, \quad (\text{C.6})$$

#### After collision

$$q_j^{l+} = A_j^{l+} \operatorname{sech} \left( \eta_{lR} + \frac{R_3 - R_{3-l}}{2} \right) e^{i\eta_{lI}}, \quad (\text{C.7})$$

$$q_3^{l+} = A_3^{l+} \left[ \cos\varphi_l \tanh \left( \eta_{lR} + \frac{R_3 - R_{3-l}}{2} \right) + i \sin\varphi_l \right], \quad j, l = 1, 2, \quad (\text{C.8})$$

where  $\eta_{lR} = k_{lR}(X - 2k_{lI}T)$ ,  $\eta_{lI} = k_{lI}X - (k_{lR}^2 - k_{lI}^2 - 2|c_1|^2)T$ ,  $A_j^{l-} = \frac{\alpha_l^{(j)}}{2} e^{-\frac{R_l}{2}}$ ,  $A_3^{l-} = -c_1 e^{i(\zeta_1 + \varphi_l)}$ ,  $A_j^{l+} = \frac{1}{2} e^{-(R_{3-l} + R_3)/2 + \delta_{lj}}$  and  $A_3^{l+} = c_1 e^{i(\zeta_1 + 2\varphi_{3-l} + \varphi_l)}$ . The quantities  $R_1, R_2, R_3$  and  $\delta_{lj}$ ,  $l, j = 1, 2$ , appearing in the above expressions are defined below Eq. (B.5) and  $\varphi_l = \tan^{-1} \left( \frac{k_{lI} - b_l}{k_{lR}} \right)$ ,  $l = 1, 2$ .

## References

- [1] Pethick C and Smith H 2002 *Bose-Einstein Condensation in Dilute Gases* (Cambridge: Cambridge University Press)
- Pitaevskii L P and Stringari S 2003 *Bose-Einstein Condensation* (Oxford: Oxford University Press)
- [2] Kevrekidis P G, Frantzeskakis D J and Carretero-González (Eds.) R 2008 *Emergent Nonlinear Phenomena in Bose-Einstein Condensates: Theory and Experiment* (Springer)
- [3] Carretero-González R, Frantzeskakis D J and Kevrekidis P G 2008 *Nonlinearity* **21** R139
- [4] Abdullaev F Kh, Gammal A, Kamchatnov A M and Tomio L 2005 *Int. J. Mod. Phys. B* **19** 3415
- [5] Frantzeskakis D J 2010 *J. Phys. A: Math. Theor.* **43** 213001
- [6] Fetter A L and Svidzinsky A A 2001 *J. Phys.: Condens. Matter* **13** R135
- Kevrekidis P G, Carretero-González R, Frantzeskakis D J and Kevrekidis I G 2004 *Mod. Phys. Lett. B* **18** 1481
- [7] Kevrekidis P G and Frantzeskakis D J 2004 *Mod. Phys. Lett. B* **18** 173
- [8] Eiermann B, Anker Th, Albiez M, Taglieber M, Treutlein P, Marzlin K P and Oberthaler M K 2004 *Phys. Rev. Lett.* **92** 230401
- [9] Myatt C J, Burt E A, Ghrist R W, Cornell E A and Wieman C E 1997 *Phys. Rev. Lett.* **78** 586
- [10] Hall D S, Matthews M R, Ensher J R, Wieman C E and Cornell E A 1998 *ibid.* **81** 1539
- [11] Busch T and Anglin J R 2001 *Phys. Rev. Lett.* **87** 010401
- [12] Becker C, Stellmer S, Soltan-Panahi P, Dörscher S, Baumert M, Richter E -M, Kronjäger J, Bongs K and Sengstock K 2008 *Nature Phys.* **4** 496
- [13] Hamner C, Chang J J, Engels P and Hofer M A 2011 *Phys. Rev. Lett.* **106** 065302
- Middelkamp S, Chang J J, Hamner C, Carretero-González R, Kevrekidis P G, Achilleos V, Frantzeskakis D J, Schmelcher P and Engels P 2011 *Phys. Lett. A* **375** 642

- Yan D, Chang J J, Hamner C, Kevrekidis P G, Engels P, Achilleos V, Frantzeskakis D J, Carretero-González R and Schmelcher P 2011 *Phys. Rev. A* **84** 053630
- [14] Hofer M A, Chang J J, Hamner C and Engels P 2011 *Phys. Rev. A* **84** 041605(R)
- [15] Ieda J, Miyakawa T and Wadati M 2004 *Phys. Rev. Lett.* **93** 194102
- [16] Ieda J, Miyakawa T and Wadati M 2004 *J. Phys. Soc. Jpn.* **73** 2996
- [17] Li L, Li Z, Malomed B A, Mihalache D and Liu W M 2005 *Phys. Rev. A* **72** 033611
- [18] Nistazakis H E, Frantzeskakis D J, Kevrekidis P G, Malomed B A and Carretero-González R 2008 *Phys. Rev. A* **77** 033612
- [19] Inouye S, Andrews M R, Stenger J, Miesner H J, Stamper-Kurn D M and W. Ketterle 1998 *Nature* **392** 151  
 Stenger J, Inouye S, Andrews M R, Miesner H -J, Stamper-Kurn D M and Ketterle W 1999 *Phys. Rev. Lett.* **82** 2422  
 Roberts J L, Claussen N R, Burke J P, Jr., Greene C H, Cornell E A and Wieman C E 1998 *ibid.* **81** 5109  
 Cornish S L, Claussen N R, Roberts J L, Cornell E A and Wieman C E 2000 *ibid.* **85** 1795  
 Donley E A, Claussen N R, Cornish S L, Roberts J L, Cornell E A and Weiman C E 2001 *Nature* **412** 295
- [20] Khaykovich L, Schreck F, Ferrari G, Bourdel T, Cubizolles J, Carr L D, Castin Y and Salomon C 2002 *Science* **296** 1290  
 Strecker K E, Partidge G B, Truscott A G and Hulet R G 2002 *Nature* **417** 150  
 Cornish S L, Thompson S T and Wieman C E 2006 *Phys. Rev. Lett.* **96** 170401
- [21] Kevrekidis P G, Theocharis G, Frantzeskakis D J and Malomed B A 2003 *Phys. Rev. Lett.* **90** 230401
- [22] Abdullaev F Kh, Caputo J G, Kraenkel R A and Malomed B A 2003 *Phys. Rev. A* **67** 013605  
 Saito H and Ueda M 2003 *Phys. Rev. Lett.* **90** 040403  
 Montesinos G D, Pérez-García V M and Torres P J 2004 *Physica D* **191** 193
- [23] Pelinovsky D E, Kevrekidis P G and Frantzeskakis D J 2003 *Phys. Rev. Lett.* **91** 240201  
 Pelinovsky D E, Kevrekidis P G, Frantzeskakis D J and Zharnitsky V 2004 *Phys. Rev. E* **70** 047604  
 Matuszewski M, Infeld E, Malomed B A and Trippenbach M 2005 *Phys. Rev. Lett.* **95** 050403
- [24] Liang Z X, Zhang Z D and Liu W M 2005 *Phys. Rev. Lett.* **94** 050402
- [25] Serkin V N, Hasegawa A and Belyaeva T L 2007 *Phys. Rev. Lett.* **98** 074102; 2012 *Phys. Rev. A* **81** 023610
- [26] Rajendran S, Lakshmanan M and Muruganandam P 2011 *J. Math. Phys.* **52** 023515  
 Rajendran S, Muruganandam P and Lakshmanan M 2010 *Physica D* **239** 366
- [27] Sheppard A P and Kivshar Y S 1997 *Phys. Rev. E* **55** 4773
- [28] Kanna T and Lakshmanan M 2001 *Phys. Rev. Lett* **86** 5043; 2003 *Phys. Rev. E* **67** 046617
- [29] Kanna T, Lakshmanan M, Tchofo Dinda P and Akhmediev N 2006 *Phys. Rev. E* **73** 026604
- [30] Deconinck B, Kevrekidis P G, Nistazakis H E and Frantzeskakis D J 2004 *Phys. Rev. A* **70** 063605
- [31] Merhasin I M, Malomed B A and Driben R 2005 *J. Phys. B: At. Mol. Opt. Phys.* **38** 877
- [32] Nistazakis H E, Rapti Z, Frantzeskakis D J, Kevrekidis P G, Sodano P and Trombettoni A 2008 *Phys. Rev. A* **78** 023635
- [33] Dudin Y O, Li L, Bariani F and Kuzmich A 2012 *Nature Phys.* **8** 790
- [34] Manakov S V 1973 *Zh. Eksp. Teor. Fiz.* **65** 1392; 1974 *Sov. Phys. -JETP* **38** 248
- [35] Williams J, Walser R, Cooper J, Cornell E A and Holland M 2000 *Phys. Rev. A* **61** 033612
- [36] Thalhammer G, Barontini G, De Sarlo L, Catani J, Minardi F and Inguscio M 2008 *Phys. Rev. Lett.* **100** 210402
- [37] Papp S B, Pino J M and Wieman C E 2008 *Phys. Rev. Lett.* **101** 040402
- [38] Zakhrov V E and Schulman E I 1982 *Physica* **4D** 270  
 Radhakrishnan R and Lakshmanan M 1995 *J. Phys. A: Math. Gen.* **28** 2683
- [39] Vijayajayanthi M, Kanna T and Lakshmanan M 2009 *Nonlinear Dynamics* ed Daniel M and

- Rajasekar S (New Delhi: Narosa Publication) pp 125-128
- [40] Vijayajayanthi M, Kanna T and Lakshmanan M 2009 *Eur. Phys. J. Special Topics* **173** 57
- [41] Hirota R 1973 *J. Math. Phys.* **14** 805
- [42] Yan D, Chang J J, Hamner C, Hofer M, Kevrekidis P G, Engels P, Achilleos V, Frantzeskakis D J and Cuevas J 2012 *J. Phys. B: At. Mol. Opt. Phys.* **45** 115301
- [43] Abdullaev F Kh and Salerno M 2003 *J Phys B: At. Mol. Opt. Phys.* **36** 2851; Ju-Kui Xue 2005 *J Phys B: At. Mol. Opt. Phys.* **38** 3841